Dyes and Pigments 82 (2009) 171–186

Contents lists available at ScienceDirect

Dyes and Pigments

journal homepage: www.elsevier.com/locate/dyepig

# The syntheses, structures and nonlinear optical and related properties of salts with julolidinyl electron donor groups

Benjamin J. Coe [a,*], Simon P. Foxon [a], Elizabeth C. Harper [a], James A. Harris [a], Madeleine Helliwell [a], James Raftery [a], Inge Asselberghs [b], Koen Clays [b], Edith Franz [b], Bruce S. Brunschwig [c], Anthony G. Fitch [c]

[a] School of Chemistry, University of Manchester, Oxford Road, Manchester M13 9PL, UK
[b] Department of Chemistry, University of Leuven, Celestijnenlaan 200D, B-3001 Leuven, Belgium
[c] Molecular Materials Research Center, Beckman Institute, MC 139-74, California Institute of Technology, 1200 East California Boulevard, Pasadena, CA 91125, USA

ARTICLE INFO

*Article history:*
Received 21 October 2008
Received in revised form
22 December 2008
Accepted 23 December 2008
Available online 3 January 2009

*Keywords:*
Organic synthesis
Nonlinear optics
Julolidinyl dyes
Hyper-Rayleigh scattering
Stark spectroscopy

ABSTRACT

Twelve, dipolar cations with 2,3,6,7-tetrahydro-1*H*,5*H*-pyrido[3,2,1-*ij*]quinolin-9-yl (julolidinyl, Jd) electron donor groups and *N*-methyl/arylpyridinium, *N*-methylquinolinium or *N*-methylbenzothiazolium acceptor groups were synthesised. The chromophores were characterised as their $PF_6^-$ salts using various techniques including electronic absorption spectroscopy and cyclic voltammetry; single crystal X-ray structures were determined for a large number of salts, all of which form nonpolar materials. A broad correlation between the electron acceptor strength and the degree of bond length alternation is evident. A key focus of this work is detailed comparisons of the Jd-containing chromophores with their previously studied 4-(dimethylamino)phenyl (Dap) analogues. Molecular, quadratic, nonlinear optical responses were determined using femtosecond hyper-Rayleigh scattering at both 1300 and 800 nm, as well as using Stark (electroabsorption) spectroscopic studies of intense, visible $\pi \rightarrow \pi^*$ intramolecular charge-transfer bands. Substantial red shifts in the latter transitions are observed on replacing Dap with Jd which indicate that the latter acts as a more effective π-electron donor. With few exceptions, both hyper-Rayleigh scattering and Stark data generally show that using Jd instead of Dap increases the static first hyperpolarizability $\beta_0$, in accord with expectations based on the two-state model. $\beta_0$ values as high as 6 times larger than that of the chromophore in the technologically important material *E*-4′-(dimethylamino)-*N*-methyl-4-stilbazolium tosylate are observed.



## 1. Introduction

Organic nonlinear optical (NLO) materials are of interest for various applications such as optical data processing and biological imaging [1]. Amongst the range of available compounds, organic salts are especially attractive due to their high stability and tailorability. The latter aspect is enhanced by possibilities for using counterion variations to modify crystal packing, aimed at producing polar structures that display bulk quadratic NLO effects such as second harmonic generation (SHG) and electro-optic (EO) behaviour. In this area, particular attention has focused on stilbazolium species, including *E*-4′-(dimethylamino)-*N*-methyl-4-stilbazolium tosylate (DAST) [2] and related compounds [3]. Due to their large EO coefficients, DAST and similar materials are useful for terahertz (THz) wave generation via nonlinear frequency mixing, of relevance to many applications such as security scanning, biomedical analysis and space communications [4]. Recent studies by Günter and colleagues have involved salts containing the chromophore of DAST combined with different arylsulfonate anions, affording a number of new materials that are highly active for SHG [3f,g,i,4g]. However, the molecular engineering of the active chromophore has received rather less attention, and there exists much scope for producing new salt compounds with enhanced NLO properties.

The molecular origin of quadratic (*second-order*) NLO effects is the first hyperpolarizability $\beta$ and this response property corresponds with the bulk susceptibility $\chi^{(2)}$ in materials. It is well established that a large $\beta$ generally derives from a polarizable π-conjugated system that bears electron-donating (D) and -accepting (A) groups [1], the latter being a pyridinium (pyd) unit in stilbazolium and related species. Such chromophores show intense linear optical absorptions due to $\pi(D) \rightarrow \pi^*(A)$ intramolecular

* Corresponding author. Tel.: +44 161 275 4601; fax: +44 161 275 4598.
*E-mail address:* b.coe@manchester.ac.uk (B.J. Coe).

0143-7208/$ – see front matter © 2008 Elsevier Ltd. All rights reserved.
doi:10.1016/j.dyepig.2008.12.010

charge-transfer (ICT), and static (*off-resonance*) first hyperpolarizabilities $\beta_0$ can be estimated via a two-state model (TSM) in cases where a single low energy ICT transition dominates the NLO response [5]. Our previous studies with stilbazolium and related salts have involved various techniques including hyper-Rayleigh scattering (HRS) [6] and electronic Stark effect (electroabsorption) spectroscopy [7], with a focus on chromophores with *N*-arylpyridinium groups [8]. This work has identified several non-centrosymmetric crystalline materials that show very large powder SHG efficiencies (similar to that of DAST) [8a,c], and one of these also shows polymorphism [9]. Furthermore, large single crystals of the compound *E*-4′-(dimethylamino)-*N*-phenyl-4-stilbazolium hexafluorophosphate (DAPSH) display a record non-resonant bulk NLO coefficient $d_{111}$ of 290 pm $V^{-1}$ at 1907 nm [10]. Other related studies include chromophores with *N*-methylbenzothiazolium A groups [11] and two-dimensional diquat systems [12]. Our present investigations focus on a series of chromophores with electron-rich 2,3,6,7-tetrahydro-1*H*,5*H*-pyrido[3,2,1-*ij*]quinolin-9-yl (julolidinyl, Jd) groups connected to *N*-quaternised electron acceptors. The Jd group has been employed previously in various NLO chromophores, but almost exclusively neutral molecules [13]. To our knowledge, there is only one existing relevant report of Jd salts which is limited in scope to powder SHG studies of salts of the cation **1** and includes no $\beta$ measurements [14]. The objectives of our present work are to realise substantially increased NLO responses by synthesising and characterising an extensive series of new charged chromophores. In addition, we use a wide range of complementary techniques to provide the first detailed, quantitative comparisons between the Jd electron donor and the more widely exploited 4-(dimethylamino)phenyl (Dap) group.

## 2. Experimental

### 2.1. Materials and procedures

The compounds *N*-methyl-4-picolinium iodide ([Mepic$^+$]I) [15], *N*-phenyl-4-picolinium chloride hydrate ([Phpic$^+$]Cl·1.25$H_2O$) [8a], *N*-(2,4-dinitrophenyl)-4-picolinium hexafluorophosphate ([DNPhpic$^+$]$PF_6$) [8a], *N*-(2-pyrimidyl)-4-picolinium hexafluorophosphate ([Pympic$^+$]$PF_6$) [8a] and 2,3-dimethylbenzothiazolium iodide ([dmbzt$^+$]I) [16] were prepared according to the literature. 2,3,6,7-Tetrahydro-1*H*,5*H*-pyrido[3,2,1-*ij*]quinoline-9-carbaldehyde (Jdca) was synthesised by following a published method [17], but using a more convenient total reaction time of 20 h (16 h followed by 4 h treatment with aqueous NaOH). Recrystallisation was ineffective, so purification involved column chromatography on silica gel with dichloromethane:methanol (95:5) as eluant, giving a yield of 77%. All other reagents were obtained commercially and used as supplied. Products were dried overnight at room temperature in a vacuum desiccator ($CaSO_4$) prior to characterisation.

### 2.2. General physical measurements

$^1$H NMR spectra were recorded on Inova 300 ([**2**]$PF_6$) and 400 ([**1**]$PF_6$, [**3**]$PF_6$, [**4**]$PF_6$, [**7**]Cl and [**10**]$BPh_4$) spectrometers, a Bruker 500 spectrometer ([Mequin$^+$]I, [Mequin$^+$]$PF_6$, Jdpa, [**5**]$PF_6$, [**6**]$PF_6$, [**6**]Cl and [**7**–**12**]$PF_6$) or a Varian Gemini 200 spectrometer ([**23**]$PF_6$), and all shifts are referenced to TMS. The fine splitting of pyridyl or phenyl ring AA′BB′ patterns is ignored and the signals are reported as simple doublets, with *J* values referring to the two most intense peaks. Elemental analyses were performed by the Microanalytical Laboratory, University of Manchester and UV−vis spectra were obtained by using a Thermo Electron Corporation Helios β v4.60 spectrophotometer. Mass spectra were recorded by using +electrospray on a Micromass Platform spectrometer. Cyclic voltammetric measurements were carried out by using an EG&G PAR model 283 potentiostat/galvanostat. A single-compartment cell was used with a silver/silver chloride reference electrode (3 M NaCl, saturated AgCl) separated by a salt bridge from a glassy carbon working electrode and Pt wire auxiliary electrode. Acetonitrile was freshly distilled (from $CaH_2$) and [N$^n$Bu$_4$]$PF_6$ was used as the supporting electrolyte. Solutions containing *ca.* $10^{-3}$ M analyte (0.1 M electrolyte) were deaerated by purging with $N_2$. All $E_{1/2}$ values were calculated from $(E_{pa}+E_{pc})/2$ at a scan rate of 200 mV $s^{-1}$.

### 2.3. Synthesis

#### 2.3.1. 1,4-Dimethylquinolinium iodide, [Mequin$^+$]I

Iodomethane (2.5 mL) was added dropwise to a stirred solution of lepidine (5.3 mL, 40.0 mmol) at 0 °C. The yellow solution was allowed to warm slowly to room temperature to give a yellow solid which was filtered off, washed with diethyl ether, chloroform and copious amounts of acetone and dried: 4.24 g, 37%; $\delta_H$ (500 MHz, $D_2O$) 8.84 (1H, d, $J=6.0$ Hz, $C_9H_6N$), 8.30 (1H, d, $J=8.5$ Hz, $C_9H_6N$), 8.17 (1H, d, $J=9.2$ Hz, $C_9H_6N$), 8.04 (1H, t, $J=7.9$ Hz, $C_9H_6N$), 7.84 (1H, t, $J=7.9$ Hz, $C_9H_6N$), 7.70 (1H, d, $J=6.3$ Hz, $C_9H_6N$), 4.41 (3H, s, $N^+$–Me), 2.84 (3H, s, Me). Anal. Calcd. (%) for $C_{11}H_{12}NI$: C, 46.34; H, 4.24; N, 4.91. Found: C, 46.07; H, 4.10; N, 4.90.

#### 2.3.2. 1,4-Dimethylquinolinium hexafluorophosphate, [Mequin$^+$]$PF_6$

[Mequin$^+$]I (2.00 g, 7.01 mmol) was dissolved in a minimum of methanol and aqueous $NH_4PF_6$ was added. The resulting white precipitate was filtered off, washed with water and dried: 1.20 g, 56%; $\delta_H$ (500 MHz, $CD_3COCD_3$) 9.19 (1H, d, $J=6.0$ Hz, $C_9H_6N$), 8.45–8.41 (2H, $C_9H_6N$), 8.24 (1H, t, $J=7.9$ Hz, $C_9H_6N$), 7.95–7.92 (2H, $C_9H_6N$), 4.63 (3H, s, $N^+$–Me), 2.94 (3H, s, Me). Anal. Calcd. (%) for $C_{11}H_{12}F_6NP$: C, 43.58; H, 3.99; N, 4.62. Found: C, 43.16; H, 3.93; N, 4.55.

#### 2.3.3. 3-(2,3,6,7-Tetrahydro-1H,5H-pyrido[3,2,1-ij]quinolin-9-yl) propenal, Jdpa

2,3,6,7-Tetrahydro-1*H*,5*H*-pyrido[3,2,1-*ij*]quinoline-9-carbaldehyde (808 mg, 4.01 mmol) and 1,3-dioxan-2-yl-tributylphosphonium bromide (6.8 mL, 1.2 M, 8.16 mmol) were dissolved in anhydrous tetrahydrofuran (100 mL). Sodium hydride (264 mg, 11.0 mmol) was added with a catalytic amount of 18-crown-6 and the suspension was stirred for 20 h at room temperature. Water (100–200 mL) was added and the organic layer was extracted with diethyl ether (3 × 100 mL). The extracts were combined and concentrated under reduced pressure to afford a yellow oil. This material was dissolved in tetrahydrofuran (30 mL), 10% hydrochloric acid (20 mL) was added and solution was stirred for 1 h at room temperature. Water (100–200 mL) was added and the organic layer was extracted with dichloromethane (5 × 100 mL). The extracts were combined and concentrated under reduced pressure to afford a yellow solid. This material was purified using column chromatography on silica gel with dichloromethane as eluant. The major orange band was collected, concentrated under reduced pressure and dried to give the product as a fine yellow powder: 535 mg, 59%; $\delta_H$ (500 MHz, $CDCl_3$) 9.47 (1H, d, $J=8.2$ Hz, CHO), 7.21–7.19 (1H, m, CH), 6.95 (2H, s, $C_6H_2$), 6.40 (1H, dd, $J=15.5$, 7.9 Hz, CH), 3.19 (4H, t, $J=5.4$ Hz, $CH_2$), 2.68 (4H, t, $J=6.0$ Hz, $CH_2$), 1.92–1.85 (m, 4H, $CH_2$). Anal. Calcd. (%) for $C_{15}H_{17}NO$: C, 79.26; H, 7.54; N, 6.16. Found: C, 78.68; H, 7.35; N, 6.15.

#### 2.3.4. E-N-Methyl-4-[2-(2,3,6,7-tetrahydro-1H,5H-pyrido[3,2,1-ij] quinolin-9-yl)vinyl]pyridinium hexafluorophosphate, [**1**]$PF_6$

Jdca (120 mg, 0.596 mmol) and [Mepic$^+$]I (143 mg, 0.608 mmol) were dissolved in methanol (15 mL). Piperidine (1 drop) was added

and the solution was heated under reflux for 4 h before being allowed to cool to room temperature. The deep red solution was reduced to 5 mL in vacuo and diethyl ether (25 mL) was added to afford a beetroot red coloured precipitate which was filtered off, washed with diethyl ether and dried. The precipitate was washed with acetone to remove any unreacted [Mepic$^+$]I and dried. The remaining solid was dissolved in a minimum of methanol (*ca.* 5 mL) and aqueous $NH_4PF_6$ was added. The resulting precipitate was filtered off, washed with water and dried: 44 mg, 17%; $\delta_H$ (400 MHz, $CD_3COCD_3$) 8.63 (2H, d, $J = 7.2$ Hz, $C_5H_4N$), 8.01 (2H, d, $J = 7.2$ Hz, $C_5H_4N$), 7.79 (1H, d, $J = 16.0$ Hz, CH), 7.16 (2H, s, $C_6H_2$), 7.07 (1H, d, $J = 16.0$ Hz, CH), 4.36 (3H, s, Me), 3.31 (4H, t, $J = 5.8$ Hz, $CH_2$), 2.73 (4H, t, $J = 6.4$ Hz, $CH_2$), 1.96–1.90 (4H, m, $CH_2$). Anal. Calcd. (%) for $C_{20}H_{23}F_6N_2P$: C, 55.05; H, 5.31; N, 6.42. Found: C, 54.84; H, 5.00; N, 6.40. *m/z*: 291 ($[M - PF_6]^+$).

*2.3.5.* E-N-*Phenyl-4-[2-(2,3,6,7-tetrahydro-1*H,5H-*pyrido[3,2,1-*ij*] quinolin-9-yl)vinyl]pyridinium hexafluorophosphate, [**2**]$PF_6$*

This compound was prepared in a manner similar to [**1**]$PF_6$ by using Jdca (100 mg, 0.497 mmol) and [Phpic$^+$]Cl·1.25$H_2O$ (102 mg, 0.447 mmol) in place of [Mepic$^+$]I to afford a sticky purple solid. This solid was dissolved in a minimum of acetone and aqueous $NH_4PF_6$ was added to afford a purple precipitate which was filtered off, washed with water and dried (crude yield 150 mg). This product was purified by vapour diffusion of diethyl ether into an acetonitrile solution, affording diffraction quality crystals: 102 mg, 40%; $\delta_H$ (300 MHz, $CD_3COCD_3$) 8.89 (2H, d, $J = 6.9$ Hz, $C_5H_4N$), 8.16 (2H, d, $J = 7.2$ Hz, $C_5H_4N$), 8.00 (1H, d, $J = 15.9$ Hz, CH), 7.89 (2H, s, Ph), 7.77 (3H, s, Ph), 7.26 (2H, s, $C_6H_2$), 7.21 (1H, d, $J = 15.9$ Hz, CH), 3.38 (4H, t, $J = 5.7$ Hz, $CH_2$), 2.78 (4H, t, $J = 6.4$ Hz, $CH_2$), 2.01–1.94 (4H, m, $CH_2$). Anal. Calcd. (%) for $C_{25}H_{25}F_6N_2P$·MeCN: C, 60.11; H, 5.23; N, 7.79. Found: C, 60.42; H, 5.22; N, 7.69. *m/z*: 353 ($[M - PF_6]^+$).

*2.3.6.* E-N-*(2,4-Dinitrophenyl)-4-[2-(2,3,6,7-tetrahydro-1*H,5H-*pyrido[3,2,1-*ij*]quinolin-9-yl)vinyl]pyridinium hexafluorophosphate, [**3**]$PF_6$*

This compound was prepared in a manner similar to [**2**]$PF_6$ by using [DNPhpic$^+$]$PF_6$ (160 mg, 0.397 mmol) in place of [Phpic$^+$]Cl·1.25$H_2O$. After concentration in vacuo, the addition of diethyl ether (50 mL) afforded a green-blue precipitate. Reprecipitation from acetone/aqueous $NH_4PF_6$ afforded the crude product (62 mg). Purification was achieved by vapour diffusion of diethyl ether into acetonitrile solution to give a dark crystalline solid: 29 mg, 12%; $\delta_H$ (400 MHz, $CD_3COCD_3$) 9.19 (1H, d, $J = 2.8$ Hz, $H^3$), 8.96 (1H, dd, $J = 8.6$, 2.8 Hz, $H^5$), 8.77 (2H, d, $J = 7.2$ Hz, $C_5H_4N$), 8.50 (1H, d, $J = 8.8$ Hz, $H^6$), 8.13 (2H, d, $J = 7.2$ Hz, $C_5H_4N$), 8.07 (1H, d, $J = 15.6$ Hz, CH), 7.28 (2H, s, $C_6H_2$), 7.21 (1H, d, $J = 15.6$ Hz, CH), 3.40 (4H, t, $J = 5.8$ Hz, $CH_2$), 2.76 (4H, t, $J = 6.4$ Hz, $CH_2$), 1.98–1.92 (4H, m, $CH_2$). Anal. Calcd. (%) for $C_{25}H_{23}F_6N_4O_4P$: C, 51.03; H, 3.94; N, 9.52. Found: C, 50.77; H, 3.90; N, 9.74. *m/z*: 443 ($[M - PF_6]^+$).

*2.3.7.* E-N-*(2-Pyrimidyl)-4-[2-(2,3,6,7-tetrahydro-1*H,5H-*pyrido [3,2,1-*ij*]quinolin-9-yl)vinyl]pyridinium hexafluorophosphate, [**4**]$PF_6$*

This compound was prepared in a manner similar to [**3**]$PF_6$ by using Jdca (80 mg, 0.397 mmol) and [Pympic$^+$]$PF_6$ (126 mg, 0.397 mmol) in place of [DNPhpic$^+$]$PF_6$. Reprecipitation from acetone/aqueous $NH_4PF_6$ afforded the pure product as a dark blue solid: 70 mg, 35%; $\delta_H$ (400 MHz, $CD_3COCD_3$) 9.60 (2H, d, $J = 7.6$ Hz, $C_5H_4N$), 9.12 (2H, d, $J = 4.8$ Hz, $C_4N_2H_3$), 8.09 (1H, d, $J = 15.6$ Hz, CH), 8.07 (2H, d, $J = 7.2$ Hz, $C_5H_4N$), 7.83 (1H, t, $J = 4.8$ Hz, $C_4N_2H_3$), 7.32 (2H, s, $C_6H_2$), 7.23 (1H, d, $J = 15.6$ Hz, CH), 3.41 (4H, t, $J = 5.8$ Hz, $CH_2$), 2.77 (4H, t, $J = 6.4$ Hz, $CH_2$), 1.99–1.93 (4H, m, $CH_2$). Anal. Calcd. (%) for $C_{23}H_{23}F_6N_4P$: C, 55.20; H, 4.63; N, 11.20. Found: C, 54.93; H, 4.57; N, 11.13. *m/z*: 355 ($[M - PF_6]^+$).

*2.3.8.* E-N-*Methyl-4-[2-(2,3,6,7-tetrahydro-1*H,5H-*pyrido[3,2,1-*ij*] quinolin-9-yl)vinyl]quinolinium hexafluorophosphate, [**5**]$PF_6$*

This compound was prepared in a manner similar to [**4**]$PF_6$ by using [Mequin$^+$]$PF_6$ (152 mg, 0.501 mmol) in place of [Pympic$^+$]$PF_6$. After the addition of diethyl ether the solution was refrigerated for 1 h, then the resulting dark blue precipitate was filtered off, washed with diethyl ether and dried. Reprecipitation from acetone/$NH_4PF_6$ afforded a dark green/blue solid: 40 mg, 16%; $\delta_H$ (500 MHz, $CD_3COCD_3$) 8.98 (1H, d, $J = 7.0$ Hz, $C_9H_6N$), 8.95 (1H, dd, $J = 7.8$, 1.5 Hz, $C_9H_6N$), 8.39 (1H, d, $J = 8.5$ Hz, $C_9H_6N$), 8.27 (1H, d, $J = 6.5$ Hz, $C_9H_6N$), 8.25–8.21 (1H, m, $C_9H_6N$), 8.09 (1H, d, $J = 15.5$ Hz, CH), 8.00–7.96 (2H, $C_9H_6N$ + CH), 7.43 (2H, s, $C_6H_2$), 4.60 (3H, s, Me), 3.40 (4H, t, $J = 5.7$ Hz, $CH_2$), 2.80 (4H, t, $J = 6.2$ Hz, $CH_2$), 2.01–1.97 (4H, m, $CH_2$). Anal. Calcd. (%) for $C_{24}H_{25}F_6N_2P$: C, 59.26; H, 5.18; N, 5.76. Found: C, 59.06; H, 5.16; N, 5.62. *m/z*: 341 ($[M - PF_6]^+$).

*2.3.9.* E-N-*Methyl-2-[2-(2,3,6,7-tetrahydro-1*H,5H-*pyrido[3,2,1-*ij*] quinolin-9-yl)vinyl]benzothiazolium hexafluorophosphate, [**6**]$PF_6$*

This compound was prepared in a manner similar to [**5**]$PF_6$ by using Jdca (121 mg, 0.601 mmol) and [dmbzt$^+$]I (146 mg, 0.501 mmol) in place of [Mequin$^+$]$PF_6$. After concentration in vacuo, the addition of diethyl ether (250 mL) to the dark purple solution yielded a purple/blue precipitate (143 mg). Reprecipitation from methanol/aqueous $NH_4PF_6$ afforded a dark blue solid: 72 mg, 29%; $\delta_H$ (500 MHz, $CD_3COCD_3$) 8.19 (1H, d, $J = 8.0$ Hz, $C_6H_4$), 8.03 (1H, d, $J = 8.4$ Hz, $C_6H_4$), 7.95 (1H, d, $J = 14.9$ Hz, CH), 7.82–7.79 (1H, m, $C_6H_4$), 7.70–7.68 (1H, m, $C_6H_4$), 7.52 (1H, d, $J = 14.9$ Hz, CH), 7.46 (2H, s, $C_6H_2$), 4.31 (3H, s, Me), 3.46 (4H, t, $J = 5.7$ Hz, $CH_2$), 2.78 (4H, t, $J = 6.2$ Hz, $CH_2$), 2.00–1.96 (4H, m, $CH_2$). Anal. Calcd. (%) for $C_{22}H_{23}F_6N_2PS$: C, 53.66; H, 4.71; N, 5.69. Found: C, 53.60; H, 4.68; N, 5.63. *m/z*: 347 ($[M - PF_6]^+$).

*2.3.10.* E-N-*Methyl-2-[2-(2,3,6,7-tetrahydro-1*H,5H-*pyrido[3,2,1-*ij*] quinolin-9-yl)vinyl]benzothiazol-3-ium chloride, [**6**]Cl*

A portion of [**6**]$PF_6$ (43 mg, 0.087 mmol) was dissolved in a minimum of acetone and a concentrated solution of [N$^n$Bu$_4$]Cl in acetone was added dropwise until a purple precipitate formed. This solid was filtered off, washed with copious amounts of acetone and dried. Purification was effected by diffusion of diethyl ether vapour into a methanol solution to give a purple crystalline solid: 14 mg, 37%; $\delta_H$ (500 MHz, $CD_3OD$) 7.91 (1H, d, $J = 7.6$ Hz, $C_6H_4$), 7.77 (1H, d, $J = 8.2$ Hz, $C_6H_4$), 7.69 (1H, d, $J = 14.8$ Hz, CH), 7.61–7.58 (1H, m, $C_6H_4$), 7.50–7.46 (1H, m, $C_6H_4$), 7.24 (2H, s, $C_6H_2$), 7.17 (1H, d, $J = 14.8$ Hz, CH), 4.00 (3H, s, Me), 3.28 (4H, t, $J = 5.7$ Hz, $CH_2$), 2.65 (4H, t, $J = 6.3$ Hz, $CH_2$), 1.87–1.83 (4H, m, $CH_2$). Anal. Calcd. (%) for $C_{22}H_{23}ClN_2S$·1.1MeOH·$H_2O$: C, 63.60; H, 6.79; N, 6.42. Found: C, 63.50; H, 6.42; N, 6.54. Aside: the crystalline sample was allowed to dry in air and the analyses are consistent with some loss of MeOH (the crystal structure shows 1.5 molecules) accompanied by absorption of atmospheric moisture, commonly observed with such hygroscopic chloride salts.

*2.3.11.* E,E-N-*Methyl-4-[4-(2,3,6,7-tetrahydro-1*H,5H-*pyrido[3,2,1-*ij*]quinolin-9-yl)buta-1,3-dienyl]pyridinium hexafluorophosphate, [**7**]$PF_6$*

This compound was prepared in a manner similar to [**1**]$PF_6$ by using Jdpa (50 mg, 0.220 mmol) in place of Jdca and [Mepic$^+$]I (52 mg, 0.221 mmol) in methanol (20 mL) and piperidine (3 drops). To the resulting dark red/purple solution after concentration, diethyl ether (500 mL) was added and the mixture was refrigerated for 1 h to afford a purple precipitate which was filtered off, washed with diethyl ether and dried. This solid was dissolved in a minimum of methanol, aqueous $NH_4PF_6$ was added and the solid was filtered off, washed with water and dried. Purification was achieved by two sequential vapour diffusions of diethyl ether into acetonitrile solutions, affording diffraction quality red crystals: 22 mg, 22%; $\delta_H$ ($CD_3CN$) 8.26 (2H, d, $J = 7.0$ Hz, $C_5H_4N$), 7.77 (2H, d, $J = 6.9$ Hz,

$C_5H_4N$), 7.63 (1H, dd, $J = 15.1$, 9.8 Hz, CH), 7.03 (2H, s, $C_6H_2$), 6.95–6.86 (2H, 2CH), 6.60 (1H, d, $J = 15.1$ Hz, CH), 4.11 (3H, s, Me), 3.27 (4H, t, $J = 5.7$ Hz, $CH_2$), 2.74 (4H, t, $J = 6.3$ Hz, $CH_2$), 1.95–1.91 (4H, m, $CH_2$). Anal. Calcd. (%) for $C_{22}H_{25}F_6N_2P$: C, 57.14; H, 5.45; N, 6.06. Found: C, 57.06; H, 5.51; N, 6.01. *m/z*: 317 ($[M - PF_6]^+$).

### 2.3.12. E,E-N-*Methyl-4-[4-(2,3,6,7-tetrahydro-1*H,5H*-pyrido[3,2,1-*ij*]quinolin-9-yl)buta-1,3-dienyl]pyridinium chloride, [**7**]Cl*

A portion of [**7**]$PF_6$ (26 mg, 0.056 mmol) was dissolved in a minimum of acetone and a concentrated solution of $[N^nBu_4]Cl$ in acetone was added dropwise until a purple precipitate formed. This solid was filtered off, washed with copious amounts of acetone and dried. Purification was achieved by vapour diffusion of diethyl ether into a methanol solution, affording diffraction quality purple-red crystals: 7 mg, 29%; $\delta_H$ ($CD_3OD$) 8.37 (2H, d, $J = 7.1$ Hz, $C_5H_4N$), 7.77 (2H, d, $J = 6.9$ Hz, $C_5H_4N$), 7.61 (1H, dd, $J = 15.4$, 9.8 Hz, CH), 6.89–6.79 (4H, 2CH + $C_6H_2$), 6.53 (1H, d, $J = 15.1$ Hz, CH), 4.10 (3H, s, Me), 3.16 (4H, t, $J = 5.8$ Hz, $CH_2$), 2.63 (4H, t, $J = 6.3$ Hz, $CH_2$), 1.88–1.82 (4H, m, $CH_2$). Anal. Calcd. (%) for $C_{22}H_{25}ClN_2 \cdot 4H_2O$: C, 62.18; H, 7.83; N, 6.59. Found: C, 61.84; H, 7.37; N, 6.15.

### 2.3.13. E,E-N-*Phenyl-4-[4-(2,3,6,7-tetrahydro-1*H,5H*-pyrido[3,2,1-*ij*]quinolin-9-yl)buta-1,3-dienyl]pyridinium hexafluorophosphate, [**8**]$PF_6$*

Jdpa (100 mg, 0.440 mmol) and [Phpic$^+$]Cl·1.25$H_2O$ (90 mg, 0.394 mmol) were dissolved in methanol (20 mL). Pyridine (10 drops) was added and the solution was heated under reflux for 20 h in the dark before being allowed to cool to room temperature. The product was obtained from the resulting dark green/blue solution in a manner similar to [**7**]$PF_6$, using initial diethyl ether (250 mL). The crude product (32 mg) was purified by a single vapour diffusion of diethyl ether into acetonitrile solution, affording diffraction quality blue crystals: 29 mg, 13%; $\delta_H$ ($CD_3CN$) 8.53 (2H, d, $J = 7.3$ Hz, $C_5H_4N$), 7.90 (2H, d, $J = 6.9$ Hz, $C_5H_4N$), 7.78 (1H, dd, $J = 15.1$, 10.4 Hz, CH), 7.71 (2H, s, Ph), 7.66 (3H, s, Ph), 7.07 (2H, s, $C_6H_2$), 7.03–6.93 (2H, 2CH), 6.67 (1H, d, $J = 15.2$ Hz, CH), 3.29 (4H, t, $J = 5.7$ Hz, $CH_2$), 2.74 (4H, t, $J = 6.4$ Hz, $CH_2$), 1.97–1.91 (4H, m, $CH_2$). Anal. Calcd. (%) for $C_{27}H_{27}F_6N_2P$: C, 61.83; H, 5.19; N, 5.34. Found: C, 61.82; H, 4.88; N, 5.32. *m/z*: 379 ($[M - PF_6]^+$).

### 2.3.14. E,E-N-*(2,4-Dinitrophenyl)-4-[4-(2,3,6,7-tetrahydro-1*H,5H*-pyrido[3,2,1-*ij*]quinolin-9-yl)buta-1,3-dienyl]pyridinium hexafluorophosphate, [**9**]$PF_6$*

This compound was prepared in a manner similar to [**8**]$PF_6$ by using Jdpa (50 mg, 0.220 mmol) and [DNPhpic$^+$]$PF_6$ (89 mg, 0.220 mmol) in place of [Phpic$^+$]Cl·1.25$H_2O$ to afford a brown solid. This solid was dissolved in a minimum of acetone and aqueous $NH_4PF_6$ was added to afford the crude product as a blue solid (22 mg). Further purification was achieved by vapour diffusion of diethyl ether into acetonitrile solution, affording a dark crystalline solid: 18 mg, 13%; $\delta_H$ ($CD_3CN$) 9.11 (1H, d, $J = 2.5$ Hz, $H^3$), 8.79 (1H, dd, $J = 8.5$, 2.6 Hz, $H^5$), 8.32 (2H, d, $J = 7.3$ Hz, $C_5H_4N$), 8.06 (1H, d, $J = 8.5$ Hz, $H^6$), 7.95–7.84 (3H, $C_5H_4N$ + CH), 7.12–6.97 (4H, $C_2H_6$ + 2CH), 6.68 (1H, d, $J = 14.8$ Hz, CH), 3.32 (4H, t, $J = 5.7$ Hz, $CH_2$), 2.75 (4H, t, $J = 6.3$ Hz, $CH_2$), 1.95–1.93 (4H, m, $CH_2$). Anal. Calcd. (%) for $C_{27}H_{25}F_6N_4O_4P$: C, 52.78; H, 4.10; N, 9.12. Found: C, 52.70; H, 3.98; N, 9.03. *m/z*: 469 ($[M - PF_6]^+$).

### 2.3.15. E,E-N-*(2-Pyrimidyl)-4-[4-(2,3,6,7-tetrahydro-1*H,5H*-pyrido [3,2,1-*ij*]quinolin-9-yl)buta-1,3-dienyl]pyridinium hexafluorophosphate, [**10**]$PF_6$*

This compound was prepared and purified in a manner similar to [**9**]$PF_6$ by using Jdpa (100 mg, 0.440 mmol) and [Pympic$^+$]$PF_6$ (140 mg, 0.441 mmol) in place of [DNPhpic$^+$]$PF_6$. From the crude product (170 mg), a dark green solid was obtained: 44 mg, 19%; $\delta_H$ ($CD_3CN$) 9.45 (2H, d, $J = 7.3$ Hz, $C_5H_4N$), 9.00 (2H, d, $J = 4.7$ Hz, $C_4N_2H_3$), 7.89–7.83 (3H, CH + $C_5H_4N$), 7.69 (1H, t, $J = 4.7$ Hz, $C_4N_2H_3$), 7.12–7.09 (3H, CH + $C_6H_2$), 6.99 (1H, dd, $J = 14.8$, 11.0 Hz, CH), 6.68 (1H, d, $J = 15.1$ Hz, CH), 3.31 (4H, t, $J = 6.0$ Hz, $CH_2$), 2.74 (4H, t, $J = 6.3$ Hz, $CH_2$), 1.95–1.93 (4H, m, $CH_2$). Anal. Calcd. (%) for $C_{25}H_{25}F_6N_4P$: C, 57.04; H, 4.79; N, 10.64. Found: C, 56.93; H, 4.59; N, 10.37. *m/z*: 381 ($[M - PF_6]^+$).

### 2.3.16. E,E-N-*(2-Pyrimidyl)-4-[4-(2,3,6,7-tetrahydro-1*H,5H*-pyrido[3,2,1-*ij*]quinolin-9-yl)buta-1,3-dienyl]pyridinium tetraphenylborate, [**10**]$BPh_4$*

A portion of [**10**]$PF_6$ (33 mg, 0.063 mmol) was dissolved in a minimum of acetone and a concentrated solution of $[N^nBu_4]Cl$ in acetone was added dropwise until a blue precipitate formed. This solid was filtered off, washed with copious amounts of acetone and dried. The solid was then dissolved in water and a solution of $NaBPh_4$ in water was added dropwise to give a blue precipitate which was filtered off, washed with water and dried: 6 mg, 13%; $\delta_H$ ($CD_3COCD_3$) 9.68 (2H, d, $J = 7.6$ Hz, $C_5H_4N$), 9.16 (2H, d, $J = 4.8$ Hz, $C_4N_2H_3$), 8.13–8.06 (3H, CH + $C_5H_4N$), 7.87 (1H, t, $J = 4.8$ Hz, $C_4N_2H_3$), 7.37–7.33 (8H, m, Ph), 7.21–7.07 (4H, 2CH + $C_6H_2$), 6.93 (8H, t, $J = 7.3$ Hz, Ph), 6.86–6.76 (5H, Ph + CH), 3.35 (4H, t, $J = 5.6$ Hz, $CH_2$), 2.75 (4H, t, $J = 6.5$ Hz, $CH_2$), 1.99–1.93 (4H, m, $CH_2$). Anal. Calcd. (%) for $C_{49}H_{45}BN_4 \cdot 0.7H_2O$: C, 82.50; H, 6.56; N, 7.85. Found: C, 82.53; H, 6.40; N, 7.75.

### 2.3.17. E,E-N-*Methyl-4-[4-(2,3,6,7-tetrahydro-1*H,5H*-pyrido[3,2,1-*ij*]quinolin-9-yl)buta-1,3-dienyl]quinolinium hexafluorophosphate, [**11**]$PF_6$*

This compound was prepared in a manner similar to [**8**]$PF_6$ by using [Mequin$^+$]$PF_6$ (126 mg, 0.416 mmol) in place of [Phpic$^+$]Cl·1.25$H_2O$. During the reaction time of 48 h, further portions of pyridine (3 drops) were added after 24 h and 32 h. Purification was effected by vapour diffusion of diethyl ether into DMF solution, returning from the crude product (30 mg) diffraction quality blue crystals: 23 mg, 11%; $\delta_H$ ($CD_3CN$) 8.60 (2H, d, $J = 7.0$ Hz, $C_9H_6N$), 8.18–8.13 (2H, $C_9H_6N$), 8.00 (1H, d, $J = 6.6$ Hz, $C_9H_6N$), 7.95–7.92 (1H, m, $C_9H_6N$), 7.87 (1H, dd, $J = 14.8$, 10.1 Hz, CH), 7.44 (1H, d, $J = 14.5$ Hz, CH), 7.12–7.02 (4H, 2CH + $C_6H_2$), 4.34 (3H, s, Me), 3.30 (4H, t, $J = 5.7$ Hz, $CH_2$), 2.75 (4H, t, $J = 6.3$ Hz, $CH_2$), 1.98–1.94 (4H, m, $CH_2$). Anal. Calcd. (%) for $C_{26}H_{27}F_6N_2P$: C, 60.94; H, 5.31; N, 5.47. Found: C, 61.00; H, 5.15; N, 5.46. *m/z*: 367 ($[M - PF_6]^+$).

### 2.3.18. E,E-N-*Methyl-2-[4-(2,3,6,7-tetrahydro-1*H,5H*-pyrido[3,2,1-*ij*]quinolin-9-yl)buta-1,3-dienyl]benzothiazolium hexafluorophosphate, [**12**]$PF_6$*

This compound was prepared in a manner similar to [**7**]$PF_6$ by using [dmbzt$^+$]I (64 mg, 0.220 mmol) in place of [Mepic$^+$]I, and pyridine (4 drops) in place of piperidine to afford a dark blue solid. Purification was achieved by reprecipitation from methanol/aqueous $NH_4PF_6$ (46 mg crude product), followed by vapour diffusion of diethyl ether into an acetonitrile solution, affording diffraction quality dark green crystals: 29 mg, 25%; $\delta_H$ ($CD_3CN$) 8.05 (1H, d, $J = 8.2$ Hz, $C_6H_4$), 7.86–7.81 (2H, CH + $C_6H_4$), 7.75 (1H, t, $J = 7.9$ Hz, $C_6H_4$), 7.64 (1H, t, $J = 7.3$ Hz, $C_6H_4$), 7.25 (1H, d, $J = 14.9$ Hz, CH), 7.11 (2H, s, $C_6H_2$), 7.04 (1H, dd, $J = 14.9$, 11.4 Hz, CH), 6.89 (1H, d, $J = 14.2$ Hz, CH), 3.99 (3H, s, Me), 3.34 (4H, t, $J = 5.7$ Hz, $CH_2$), 2.73 (4H, t, $J = 6.3$ Hz, $CH_2$), 1.99–1.91 (4H, m, $CH_2$). Anal. Calcd. (%) for $C_{24}H_{25}F_6N_2PS$: C, 55.60; H, 4.86; N, 5.40. Found: C, 55.58; H, 4.69; N, 5.44. *m/z*: 373 ($[M - PF_6]^+$).

### 2.3.19. E,E-N-*Methyl-4-[4-(4-dimethylaminophenyl)buta-1,3-dienyl]quinolinium hexafluorophosphate, [**23**]$PF_6$*

A solution of [Mequin$^+$]I (244 mg, 0.816 mmol), 4-(dimethylamino)cinnamaldehyde (200 mg, 1.14 mmol) and pyridine (2 drops)

in methanol (30 mL) was heated under reflux for 16 h in the dark. The product was obtained in a manner similar to [**8**]$PF_6$, but by washing with methanol after aqueous precipitation to afford a dark blue solid: 210 mg, 56%; $\delta_H$ ($CD_3COCD_3$) 9.13 (1H, d, $J = 6.6$ Hz, $C_9H_6N$), 8.81 (1H, d, $J = 8.4$ Hz, $C_9H_6N$), 8.47 (1H, d, $J = 9.1$ Hz, $C_9H_6N$), 8.33–8.24 (2H, $C_9H_6N$), 8.13–8.00 (2H, CH + $C_9H_6N$), 7.72 (1H, d, $J = 15.0$ Hz, CH), 7.51 (2H, d, $J = 9.0$ Hz, $C_6H_4$), 7.33–7.13 (2H, CH), 6.78 (2H, d, $J = 9.0$ Hz, $C_6H_4$), 4.68 (3H, s, Me), 3.07 (s, 6H, $NMe_2$). Anal. Calcd. (%) for $C_{22}H_{23}F_6N_2P$: C, 57.39; H, 5.04; N, 6.08. Found: C, 57.22; H, 4.79; N, 6.03. *m/z*: 315 ($[M - PF_6]^+$).

### 2.4. X-ray crystallographic studies

Crystals of Jdca were grown by diffusion of *n*-pentane vapour into a dichloromethane solution, while those of Jdpa were grown by diffusion of *n*-hexane vapour into an ethyl acetate solution. The salts [**1**]$PF_6$, [**2**]$PF_6$·MeCN and [**3**–**5**]$PF_6$ were crystallised by diffusion of diethyl ether vapour into acetonitrile solutions and those of [**6**]Cl·1.5MeOH were grown by slow evaporation of a methanol solution. Crystals of [**10**]$BPh_4$ were grown by diffusion of diethyl ether vapour into a dichloromethane solution. Crystals of [**7**–**9**]$PF_6$, [**11**]$PF_6$ and [**12**]$PF_6$ were obtained as described above, while the two forms of [**7**]Cl, [**7**]Cl·$2H_2O$ and [**7**]Cl·1.33MeOH·$0.33H_2O$, were both crystallised by diffusion of methanol vapour into aqueous solutions. All crystallisations were carried out at room temperature. Because the crystals of [**10**]$BPh_4$ diffracted extremely weakly, the data in this case were collected using a wavelength of 0.6945 Å on Station 9.8 at the Synchrotron Radiation Source, Daresbury Laboratory, Warrington, Cheshire, UK. All other data were collected on a Bruker APEX CCD X-ray diffractometer by using graphite-monochromated, MoK$\alpha$ radiation (wavelength = 0.71073 Å). Data processing was carried out by using the Bruker SAINT [18] software package and semi-empirical absorption corrections were applied by using SADABS or TWINABS [18]. The structures were solved by direct methods and refined by full-matrix least-squares on all $F_0^2$ data using SHELXS-97 [19] and SHELXL97 [20], respectively. All non-hydrogen atoms were refined anisotropically, with hydrogen atoms bonded to carbon included in calculated positions using the riding method. All other calculations were carried out by using the SHELXTL package [21].

The asymmetric unit of [**1**]$PF_6$ contains two independent chromophoric cations and two $PF_6^-$ anions. The crystal was twinned with the second domain rotated by 180° about the real 1 0 0 axis and the twin law is (1.003 −0.006 0.002/0.911 −1.003 0.001/0.039 0 −1). The twin fraction refined to a value of 0.497(1). Twinning was also present in the crystal of [**3**]$PF_6$ and after processing in SAINT, equivalent reflections were merged using TWINABS [22]. The asymmetric unit of [**6**]Cl·1.5MeOH contains four independent cations and four $Cl^-$ anions, together with six methanol molecules. The asymmetric unit of [**12**]$PF_6$ contains two independent chromophoric cations and two $PF_6^-$ anions, while that of [**7**]Cl·$2H_2O$ contains two independent cations and two $Cl^-$ anions, together with four water molecules. The asymmetric unit of [**7**]Cl·1.33MeOH·$0.33H_2O$ contains three independent cations and three $Cl^-$ anions, together with four methanol (one of which is disordered) and one water molecules. For [**11**]$PF_6$, the structure was solved by direct methods initially in $P2_1$ because twinning had obscured the systemic absences for the *c* glide. After the twinning had been identified using *CELL_NOW* [23], the true space group $P2_1/c$ was assigned. Crystallographic data and refinement details are presented in Table 1.

### 2.5. Hyper-Rayleigh scattering

The apparatus and experimental procedures used for the fs HRS studies with high-frequency demodulation of multi-photon fluorescence were exactly as described previously [24]. All measurements were carried out in acetonitrile and the reference compounds were Disperse Red 1 ($\beta_{zzz,1300} = 86 \times 10^{-30}$ esu in acetonitrile; from the value of $54 \times 10^{-30}$ esu in chloroform, corrected for local field factors at optical frequencies) or crystal violet (octupolar $\beta_{xxx,800} = 500 \times 10^{-30}$ esu in acetonitrile; from the value of $340 \times 10^{-30}$ esu in methanol, corrected for local field factors at optical frequencies). The different nature of the reference tensor component for crystal violet has been taken into account in deriving the dipolar $\beta_{zzz}$ values for the compounds studied. Dilute solutions ($10^{-5}$–$10^{-6}$ M) were used to ensure a linear dependence of $I_{2\omega}/I_\omega^2$ on concentration, precluding the need for Lambert–Beer correction factors. The absence of demodulation at both 800 and 1300 nm, *i.e.* constant values of $\beta$ versus frequency, showed that no fluorescence contributions to the HRS signals were present at these measurement wavelengths. This situation may indicate: (i) a lack of fluorescence, (ii) spectral filtering out of fluorescence, or (iii) the fluorescence lifetime is too short for its demodulation to be observed within the bandwidth of the instrument. The reported $\beta$ values are the averages taken from measurements at different amplitude modulation frequencies.

### 2.6. Stark spectroscopy

The Stark apparatus, experimental methods and data collection procedure were as previously reported [25], except that a Xe arc lamp was used as the light source in the place of a W filament bulb. The Stark spectrum for each compound was measured at least twice. The data analysis for [**1**–**5**]$PF_6$ and [**7**–**11**]$PF_6$ was carried out as previously described [25], by using the zeroth, first and second derivatives of the absorption spectrum for analysis of the Stark $\Delta\varepsilon(\nu)$ spectrum. For [**6**]$PF_6$ and [**12**]$PF_6$, the absorption spectrum was also modeled with two Gaussian curves the first and second derivatives of which were used for analysis of the Stark $\Delta\varepsilon(\nu)$ spectrum in terms of the Liptay treatment [7]. The dipole moment change, $\Delta\mu_{12} = \mu_e - \mu_g$, where $\mu_e$ and $\mu_g$ are the respective excited and ground-state dipole moments, associated with each of the optical transitions considered in the fit was then calculated from the coefficient of the second derivative component. Butyronitrile was used as the glassing medium, for which the local field correction $f_{int}$ is estimated as 1.33 [25]. A two-state analysis of the ICT transitions gives

$$\Delta\mu_{ab}^2 = \Delta\mu_{12}^2 + 4\mu_{12}^2 \quad (1)$$

where $\Delta\mu_{ab}$ is the dipole moment change between the diabatic states and $\Delta\mu_{12}$ is the observed (adiabatic) dipole moment change. The value of $\mu_{12}$ can be determined from the oscillator strength $f_{os}$ of the transition by

$$|\mu_{12}| = \left[f_{os}/\left(1.08 \times 10^{-5} E_{max}\right)\right]^{1/2} \quad (2)$$

where $E_{max}$ is the energy of the ICT maximum (in wavenumbers) and $\mu_{12}$ is in Debyes. The degree of delocalisation $c_b^2$ and electronic coupling matrix element $H_{ab}$ for the diabatic states are given by

$$c_b^2 = \frac{1}{2}\left[1 - \left(\frac{\Delta\mu_{12}^2}{\Delta\mu_{12}^2 + 4\mu_{12}^2}\right)^{1/2}\right] \quad (3)$$

$$|H_{ab}| = \left|\frac{E_{max}(\mu_{12})}{\Delta\mu_{ab}}\right| \quad (4)$$

If the hyperpolarizability $\beta_0$ tensor has only nonzero elements along the ICT direction, then this quantity is given by

**Table 1**
Crystallographic data and refinement details for Jdca, Jdpa and the salts [**1**]$PF_6$, [**2**]$PF_6$·MeCN, [**3**–**5**]$PF_6$, [**6**]Cl·1.5MeOH, [**7**–**9**]$PF_6$, [**7**]Cl·$2H_2O$, [**7**]Cl·1.33MeOH·0.33$H_2O$, [**10**]$BPh_4$, [**11**]$PF_6$ and [**12**]$PF_6$.

| | Jdca | Jdpa | [**1**]$PF_6$ | [**2**]$PF_6$ •MeCN | [**3**]$PF_6$ | [**4**]$PF_6$ | [**5**]$PF_6$ |
|---|---|---|---|---|---|---|---|
| formula | $C_{13}H_{15}NO$ | $C_{15}H_{17}NO$ | $C_{20}H_{23}F_6N_2P$ | $C_{27}H_{28}F_6N_3P$ | $C_{25}H_{23}F_6N_4O_4P$ | $C_{23}H_{23}F_6N_4P$ | $C_{24}H_{25}F_6N_2P$ |
| $M_W$ | 201.26 | 227.30 | 436.37 | 539.49 | 588.44 | 500.42 | 486.43 |
| cryst syst | monoclinic | monoclinic | triclinic | triclinic | monoclinic | triclinic | monoclinic |
| space group | *Cc* | $P2_1/c$ | $P\bar{1}$ | $P\bar{1}$ | $P2_1/c$ | $P\bar{1}$ | $P2_1/n$ |
| *a* (Å) | 7.880(3) | 8.0090(6) | 8.8796(18) | 7.5960(19) | 11.905(2) | 8.2680(12) | 13.811(2) |
| *b* (Å) | 16.824(6) | 19.5170(16) | 11.771(2) | 13.041(3) | 24.111(5) | 11.1340(15) | 10.0652(15) |
| *c* (Å) | 8.634(3) | 8.2620(7) | 19.415(4) | 14.642(5) | 8.7400(17) | 12.4410(17) | 16.251(3) |
| $\alpha$ (deg) | | | 85.88(3) | 63.649(3) | | 80.680(2) | |
| $\beta$ (deg) | 115.387(6) | 118.3080(10) | 89.20(3) | 76.854(6) | 103.12(3) | 72.126(2) | 102.576(2) |
| $\gamma$ (deg) | | | 70.18(3) | 86.638(4) | | 85.302(2) | |
| *U* ($Å^3$) | 1034.1(7) | 1137.00a(16) | 1904.0(7) | 1264.2(6) | 2443.3(8) | 1075.0(3) | 2204.8(6) |
| *Z* | 4 | 4 | 4 | 2 | 4 | 2 | 4 |
| $D_{calcd}$ (Mg $m^{-3}$) | 1.293 | 1.328 | 1.522 | 1.417 | 1.600 | 1.546 | 1.465 |
| *T* (K) | 100(2) | 100(2) | 100(2) | 100(2) | 100(2) | 100(2) | 100(2) |
| $\mu$ ($mm^{-1}$) | 0.082 | 0.083 | 0.211 | 0.175 | 0.201 | 0.200 | 0.190 |
| crystal size ($mm^3$) | 0.25 × 0.20 × 0.15 | 0.35 × 0.25 × 0.20 | 0.40 × 0.20 × 0.05 | 0.33 × 0.25 × 0.20 | 0.40 × 0.30 × 0.20 | 0.25 × 0.15 × 0.05 | 0.35 × 0.30 × 0.05 |
| crystal appearance | colorless wedge | yellow plate | red plate | dark green block | dark brown plate | black plate | black plate |
| scan type | $\phi + \omega$ | $\phi + \omega$ | $\phi + \omega$ | $\phi + \omega$ | $\phi + \omega$ | $\phi + \omega$ | $\phi + \omega$ |
| no. of reflns collected | 1865 | 9671 | 6868 | 7388 | 5872 | 9275 | 14,956 |
| no. of independent reflns ($R_{int}$) | 1047 (0.0403) | 2679 (0.0372) | 6868 (0.0000) | 4805 (0.0915) | 5917 (0.0000) | 4873 (0.0664) | 3884 (0.0607) |
| GOF on $F^2$ | 1.149 | 0.947 | 0.830 | 0.905 | 0.994 | 0.768 | 1.065 |
| Final *R*1, *wR*2 [$I > 2\sigma(I)$][a] | 0.0789, 0.1794 | 0.0381, 0.0933 | 0.0488, 0.0983 | 0.0670, 0.1504 | 0.0669, 0.1662 | 0.0506, 0.0820 | 0.0588, 0.1578 |
| (all data) | 0.1055, 0.1897 | 0.0533, 0.0980 | 0.1188, 0.1148 | 0.1322, 0.1762 | 0.1049, 0.1830 | 0.1315, 0.0979 | 0.0835, 0.1670 |
| peak and hole (e $Å^{-3}$) | 0.321, −0.316 | 0.328, −0.256 | 1.024, −0.473 | 0.651, −0.367 | 1.457, −0.632 | 0.332, −0.302 | 0.915, −0.409 |

$$\beta_0 = \frac{3\Delta\mu_{12}(\mu_{12})^2}{(E_{max})^2} \quad (5)$$

A relative error of ±20% is estimated for the $\beta_0$ values derived from the Stark data and using Eq. (5), while experimental errors of ±10% are estimated for $\mu_{12}$, $\Delta\mu_{12}$ and $\Delta\mu_{ab}$, ±15% for $H_{ab}$ and ±50% for $c_b^2$.

## 3. Results and discussion

### 3.1. Synthesis and characterisation

We have previously investigated the $PF_6^-$ salts of the stilbazolium cations **13**–**16**, the related species **17** and **18** and their extended homologues (**19**–**22** and **24**) (Fig. 1) [8,11]. The salts [**1**–**12**]$PF_6$ have been prepared primarily to allow quantitative comparisons of the relative π-electron-donating abilities of the Jd and Dap groups, but also to identify new highly active chromophores and as a potential route to new NLO materials. Cations **1** and **6** are known as their iodide, tosylate and other salts [26,27], but their $PF_6^-$ salts are new to our knowledge. The cation **17** is known in the patent literature [27a,28], but its $PF_6^-$ salt is new. The chromophores **2**–**5** and **7**–**12** have apparently not been reported previously. The cations **1**–**12** are all synthesised via Knoevenagel-type condensations of the appropriate methyl-substituted cation with Jdca, affording relatively low isolated yields in all cases (up to 40%). It appears likely that the generally considerably higher yields (up to 96%) obtained for the related Dap compounds are a result of using *ca.* 2 equiv of 4-(dimethylamino)benzaldehyde to react with the methyl-substituted cation [8a,f,11]. The 5-fold higher yield of [**23**]$PF_6$ when compared with [**11**]$PF_6$ provides further confirmation of this hypothesis (although only 1.4 equiv of aldehyde was used in the former case). In contrast, in the syntheses of [**1**–**12**]$PF_6$ we used only *ca.* 1 equiv of Jdca because this is not a commercial compound. Condensations of 4-(dimethylamino)cinnamaldehyde with the appropriate picolinium salts failed to produce [**20**–**22**]$PF_6$, giving only the stilbazolium species due to carbanion attack at the β-vinyl carbon, rather than at the carbonyl group [8c]. However, these reactions were carried out with piperidine as the base. We have since discovered that using the weaker base pyridine can help to avoid unwanted products [11], and have adopted this approach to access [**8**–**12**]$PF_6$. Notably, the condensations of extended aldehydes with [Mepic$^+$]I give the desired products even when using piperidine [8c]. All of [**1**–**12**]$PF_6$ show diagnostic $^1$H NMR spectra, and +electrospray mass spectra and elemental analyses further confirm their identity and purity.

### 3.2. $^1$H NMR spectroscopy

Selected $^1$H NMR data for the two pyd series [**1**–**4**]$PF_6$ and [**7**–**10**]$PF_6$ are shown in Table 2, together with previously reported data for their Dap analogues [**13**–**16**]$PF_6$ and [**19**–**22**]$PF_6$ [8c], arranged to facilitate comparisons. Within both of the new series, the lowest field doublet attributed to the protons adjacent to the quaternised N atom shifts steadily downfield as the pyd unit becomes more electron deficient, as noted previously for [**13**–**16**]$PF_6$ in $CD_3CN$ [8a]. The total shift between the two extremes is *ca.* 0.9 ppm for both $n = 1$ series, but a little larger at *ca.* 1.2 ppm for both $n = 2$ series. The ethylenic protons in the $n = 1$ compounds show a similar trend, and comparisons with their Dap counterparts show that the Jd group exerts a substantial relative shielding influence (of up to *ca.* 0.2 ppm), implying a stronger electron-donating ability. The protons of the *E*,*E*-1,3-butadienyl bridges are generally similarly affected, but with some exceptions. The two higher field multiplet and doublet signals shift to lower field in every case upon replacing Dap with Jd, but the low field doublet of doublets is completely insensitive to the D group. These observations indicate, perhaps counterintuitively, that the latter signal is attributable to the proton nearest to the A group. The greater shielding effect of the Jd group is also evident, although less strongly so, in the signals for the more remote pyd protons.

### 3.3. Electronic spectroscopy

The UV–vis absorption spectra of salts [**1**–**12**]$PF_6$ and [**23**]$PF_6$ have been measured in acetonitrile and the results are presented in Table 3. The ICT data are collected together with that reported

| [**6**]Cl•1.5MeOH | [**7**]$PF_6$ | [**7**]Cl•2$H_2O$ | [**7**]Cl•1.33MeOH •0.33$H_2O$ | [**8**]$PF_6$ | [**9**]$PF_6$ | [**10**]$BPh_4$ | [**11**]$PF_6$ | [**12**]$PF_6$ |
|---|---|---|---|---|---|---|---|---|
| $C_{47}H_{58}Cl_2N_4O_3S_2$ | $C_{22}H_{25}F_6N_2P$ | $C_{22}H_{29}ClN_2O_2$ | $C_{23.33}H_{31}ClN_2O_{1.67}$ | $C_{27}H_{27}F_6N_2P$ | $C_{27}H_{25}F_6N_4O_4P$ | $C_{49}H_{45}BN_4$ | $C_{26}H_{27}F_6N_2P$ | $C_{24}H_{25}F_6N_2PS$ |
| 861.99 | 462.41 | 388.92 | 401.62 | 524.48 | 614.48 | 700.70 | 512.47 | 518.49 |
| triclinic | triclinic | triclinic | triclinic | monoclinic | triclinic | orthorhombic | monoclinic | monoclinic |
| $P\bar{1}$ | $P\bar{1}$ | $P\bar{1}$ | $P\bar{1}$ | $P2_1/n$ | $P\bar{1}$ | $P2_12_12_1$ | $P2_1/c$ | $P2_1/c$ |
| 15.9240(9) | 9.0000(10) | 9.786(2) | 14.270(2) | 15.3740(12) | 9.6500(9) | 9.740(3) | 9.0010(10) | 14.8003(16) |
| 17.3009(10) | 10.2080(11) | 14.800(3) | 14.448(2) | 9.5230(7) | 11.3500(11) | 14.143(5) | 9.6250(10) | 26.868(3) |
| 17.3589(10) | 12.2790(13) | 15.822(3) | 17.193(3) | 17.1780(13) | 13.1960(13) | 27.564(9) | 27.769(3) | 11.4199(12) |
| 90.3770(10) | 74.261(2) | 110.411(3) | 73.015(3) | | 88.819(2) | | | |
| 115.3530(10) | 74.832(2) | 96.231(4) | 74.818(3) | 104.3800(10) | 71.0110(10) | | 106.006(4) | 104.074(2) |
| 98.1540(10) | 88.751(2) | 106.381(3) | 72.418(3) | | 78.279(2) | | | |
| 4265.9(4) | 1046.5(2) | 2005.1(8) | 3172.6(9) | 2436.2(3) | 1336.6(2) | 3797(2) | 2312.5(4) | 4404.9(8) |
| 4 | 2 | 4 | 6 | 4 | 2 | 4 | 4 | 8 |
| 1.342 | 1.467 | 1.288 | 1.261 | 1.430 | 1.527 | 1.226 | 1.472 | 1.564 |
| 100(2) | 100(2) | 100(2) | 100(2) | 100(2) | 100(2) | 150(2) | 100(2) | 100(2) |
| 0.297 | 0.196 | 0.210 | 0.200 | 0.178 | 0.188 | 0.071 | 0.186 | 0.287 |
| 0.25 × 0.20 × 0.20 | 0.25 × 0.20 × 0.15 | 0.60 × 0.40 × 0.10 | 0.40 × 0.18 × 0.08 | 0.30 × 0.25 × 0.15 | 0.40 × 0.25 × 0.10 | 0.20 × 0.05 × 0.01 | 0.40 × 0.35 × 0.20 | 0.40 × 0.20 × 0.08 |
| red rod | red plate | black plate | black plate | dark green plate | yellow plate | gold needle | dark green plate | black plate |
| $\phi + \omega$ | $\phi + \omega$ | $\phi + \omega$ | $\phi + \omega$ | $\phi + \omega$ | $\phi + \omega$ | $\phi + \omega$ | $\phi + \omega$ | $\phi + \omega$ |
| 25,037 | 9059 | 13,631 | 20,828 | 20,386 | 11,635 | 19,976 | 11,250 | 22,515 |
| 17,076 (0.0311) | 4740 (0.0485) | 6957 (0.1181) | 10,854 (0.0611) | 5784 (0.0572) | 6080 (0.0551) | 2491 (0.0857) | 11,372 (0.0000) | 7781 (0.0841) |
| 0.930 | 0.776 | 1.023 | 0.788 | 0.865 | 1.053 | 1.145 | 0.878 | 0.863 |
| 0.0452, 0.1001 | 0.0446, 0.0790 | 0.0577, 0.1431 | 0.0579, 0.1231 | 0.0592, 0.1409 | 0.0444, 0.1288 | 0.0490, 0.1096 | 0.0474, 0.0784 | 0.0477, 0.1056 |
| 0.0730, 0.1111 | 0.1038, 0.0899 | 0.1083, 0.1714 | 0.1318, 0.1441 | 0.1375, 0.1606 | 0.0576, 0.1347 | 0.0657, 0.1171 | 0.0800, 0.0846 | 0.0989, 0.1153 |
| 0.895, −0.474 | 0.317, −0.233 | 0.360, −0.273 | 0.405, −0.301 | 0.630, −0.339 | 1.573, −0.352 | 0.152, −0.128 | 0.651, −0.486 | 0.597, −0.502 |

[a] The structures were refined on $F_o^2$ using all data; the values of $R1$ are given for comparison with older refinements based on $F_o$ with a typical threshold of $F_o > 4\sigma(F_o)$.

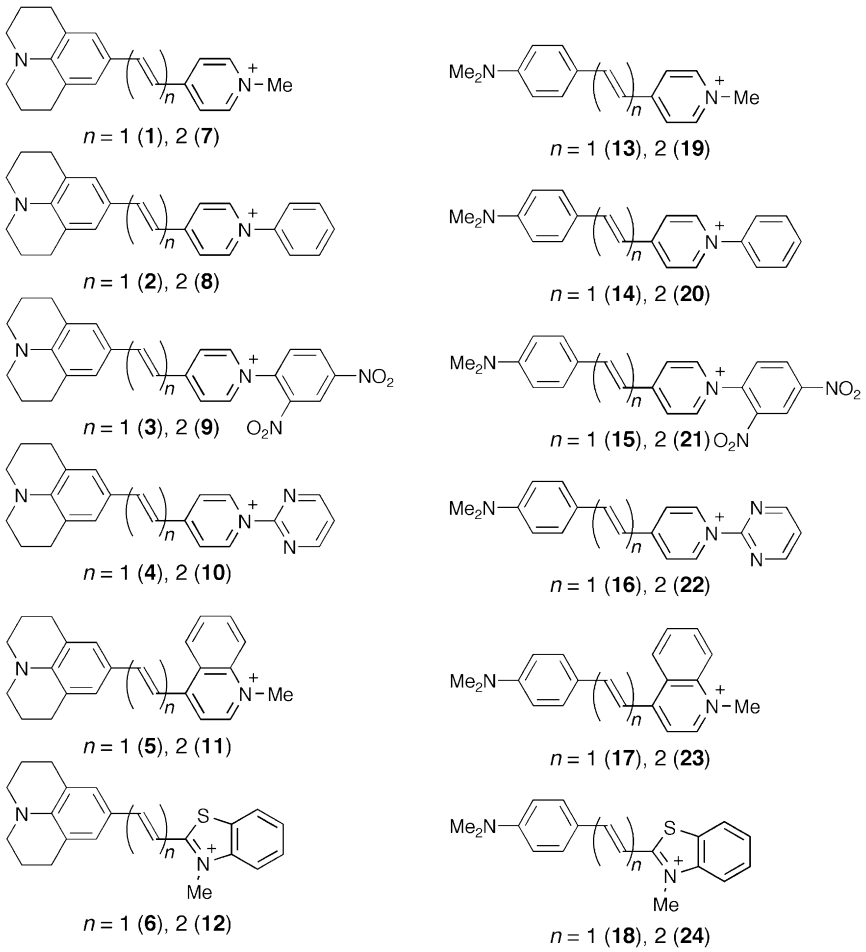


**Fig. 1.** Chemical structures of the chromophoric cations investigated; except for some of the X-ray crystal structure determinations, all of the measurements were made using $PF_6^-$ salts.

**Table 2**
Selected $^1$H NMR[a] data for salts [**1**–**4**]$PF_6$, [**7**–**10**]$PF_6$, [**13**–**16**]$PF_6$ and [**19**–**22**]$PF_6$.

| salt | δ[CH][b] (ppm) | δ[py-H][c] (ppm) |
|---|---|---|
| [**1**]$PF_6$ | 7.79, 7.07 | 8.63 |
| [**13**]$PF_6$ | 7.93, 7.20 | 8.70 |
| [**2**]$PF_6$ | 8.00, 7.21 | 8.89 |
| [**14**]$PF_6$ | 8.11, 7.33 | 8.96 |
| [**3**]$PF_6$ | 8.07, 7.21 | 9.19 |
| [**15**]$PF_6$ | 8.23, 7.38 | 9.23 |
| [**4**]$PF_6$ | 8.09, 7.23 | 9.60 |
| [**16**]$PF_6$ | *ca.* 8.11, 7.27 | 9.64 |
| [**7**]$PF_6$ | 7.63, 6.95–6.86, 6.60 | 8.26 |
| [**19**]$PF_6$[d] | 7.63, 7.08–6.89, 6.66 | 8.29 |
| [**8**]$PF_6$ | 7.78, 7.03–6.93, 6.67 | 8.53 |
| [**20**]$PF_6$[d] | 7.79, 7.17–7.07, *ca.* 6.75 | 8.58 |
| [**9**]$PF_6$ | *ca.* 7.90, *ca.* 7.12–6.97, 6.68 | 9.11 |
| [**21**]$PF_6$[d] | 7.89, 7.25–7.01, *ca.* 6.78 | 9.12 |
| [**10**]$PF_6$ | *ca.* 7.86, *ca.* 7.12–6.99, 6.68 | 9.45 |
| [**22**]$PF_6$[d] | 7.86, 7.21–6.96, 6.76 | 9.51 |

[a] In $CD_3COCD_3$ for $n = 1$ and $CD_3CN$ for $n = 2$, quoted with respect to TMS (field 200–500 MHz).
[b] Doublet signals for protons of *E*-ethenyl or *E,E*-1,3-butadienyl bridge (where resolved; estimated values are given in cases of signal overlap). In all cases where $n = 2$ the signals appear as a doublet of doublets to low field, a doublet at high field and a multiplet in between.
[c] Doublet signal for protons ortho to pyd N atom.
[d] Data taken from ref. [8c].

previously for [**13**–**22**]$PF_6$ [8a,c] and [**24**]$PF_6$ [11] in Table 4. These spectra are dominated by intense, low energy π(Jd) → π*(A) [A = pyd, quinolinium (quin) or benzothiazolium (bzt)] ICT bands in the visible region and also feature less intense bands due to nondirectional π → π* transitions at higher energies. Representative spectra of [**1**]$PF_6$, [**7**]$PF_6$, [**8**]$PF_6$, [**11**]$PF_6$ and [**19**]$PF_6$ are shown in Figs. 2 and 3.

The ICT energies $E_{max}$ of the Jd chromophores are considerably lower than those of their Dap analogues, indicating that the Jd unit is the stronger electron donor. These observations are consistent with the $^1$H NMR data (see above), and also with the results of recent density functional theoretical studies on a range of arylamino D groups [29]. For a given A group with $n = 1$, the difference in $E_{max}$ on replacing Dap with Jd is remarkably constant at *ca.* 0.22 eV, except for the bzt compounds [**6**]$PF_6$ and [**18**]$PF_6$, for which the energy shift is slightly smaller at *ca.* 0.19 eV. For the extended species, the $E_{max}$ values of the Jd chromophores are *ca.* 0.22–0.26 eV lower than those of their Dap counterparts (Fig. 2). Within both $n = 1$ series, the ICT band moves to lower energy as the electron-accepting ability of the quaternised unit increases, in the order Mepyd < Phpyd < Mebzt < DNPhpyd ≈ Mequin < Pympyd (DNPh = 2,4-dinitrophenyl, Pym = 2-pyrimidyl), with a difference in $E_{max}$

**Table 3**
UV–vis absorption data for salts [**1**–**12**]$PF_6$ and [**23**]$PF_6$ in acetonitrile.[a]

| salt | $\lambda_{max}$, nm (ε, $10^3$ $M^{-1}$ $cm^{-1}$) | $E_{max}$ (eV) | assignment |
|---|---|---|---|
| [**1**]$PF_6$ | 512 (47.0) | 2.42 | ICT |
| | 300 (11.0) | 4.13 | π → π* |
| [**2**]$PF_6$ | 554 (55.2) | 2.24 | ICT |
| | 325 (12.8) | 3.82 | π → π* |
| [**3**]$PF_6$ | 594 (57.6) | 2.09 | ICT |
| | 319 (9.1) | 3.89 | π → π* |
| [**4**]$PF_6$ | 613 (73.6) | 2.02 | ICT |
| | 325 (11.2) | 3.82 | π → π* |
| [**5**]$PF_6$ | 596 (47.2) | 2.08 | ICT |
| | 311 (13.6) | 3.99 | π → π* |
| [**6**]$PF_6$ | 566 (81.9) | 2.19 | ICT |
| | 306 (9.3) | 4.05 | π → π* |
| [**7**]$PF_6$ | 533 (47.5) | 2.33 | ICT |
| | 333 (13.7) | 3.72 | π → π* |
| | 274 (9.1) | 4.53 | π → π* |
| [**8**]$PF_6$ | 579 (58.8) | 2.14 | ICT |
| | 349 (14.7) | 3.55 | π → π* |
| | 279 (7.2) | 4.44 | π → π* |
| [**9**]$PF_6$ | 639 (63.0) | 1.94 | ICT |
| | 356 (12.6) | 3.48 | π → π* |
| [**10**]$PF_6$ | 661 (68.4) | 1.88 | ICT |
| | 374 (13.0) | 3.32 | π → π* |
| | 272 (18.3) | 4.56 | π → π* |
| [**11**]$PF_6$ | 621 (48.9) | 2.00 | ICT |
| | 339 (12.8) | 3.66 | π → π* |
| [**12**]$PF_6$ | 631 (82.1) | 1.97 | ICT |
| | 353 (9.7) | 3.51 | π → π* |
| [**23**]$PF_6$ | 560 (43.9) | 2.21 | ICT |
| | 330 (15.2) | 3.76 | π → π* |
| | 246 (17.1) | 5.04 | π → π* |

[a] Solutions *ca.* $10^{-5}$ M.

**Table 4**
ICT absorption and electrochemical data for salts [**1**–**24**]$PF_6$ in acetonitrile.

| salt | $\lambda_{max}$, nm (ε, $10^3$ $M^{-1}$ $cm^{-1}$)[a] | $E_{max}$ (eV)[a] | *E*, V *vs* Ag–AgCl (Δ$E_p$, mV)[b] | | | |
|---|---|---|---|---|---|---|
| | | | oxidation | | | reduction[c] |
| | | | $E_{pa}$ | $E_{pc}$ | $E_{1/2}$ | |
| [**1**]$PF_6$ | 512 (47.0) | 2.42 | 0.77[d] | | | −1.16 |
| [**2**]$PF_6$ | 554 (55.2) | 2.24 | 0.72 | 0.64 | | −0.94 |
| [**3**]$PF_6$ | 594 (57.6) | 2.09 | 0.80[d] | | | −0.57 |
| [**4**]$PF_6$ | 613 (73.6) | 2.02 | 0.76 | 0.67 | | −0.73 |
| [**5**]$PF_6$ | 596 (47.2) | 2.08 | | | 0.68 (90) | −0.83 |
| [**6**]$PF_6$ | 566 (81.9) | 2.19 | | | 0.81 (70) | −0.90 |
| [**7**]$PF_6$ | 533 (47.5) | 2.33 | 0.57[d] | | | −1.02 |
| [**8**]$PF_6$ | 579 (58.8) | 2.14 | 0.59[d] | | | −0.82 |
| [**9**]$PF_6$ | 639 (63.0) | 1.94 | 0.62[d] | | | −0.51 |
| [**10**]$PF_6$ | 662 (68.4) | 1.88 | 0.63[d] | | | −0.61 |
| [**11**]$PF_6$ | 621 (48.9) | 2.00 | 0.60[d] | | | −0.75 |
| [**12**]$PF_6$ | 631 (82.1) | 1.97 | | | 0.64 (90) | −0.72 |
| [**13**]$PF_6$[e] | 470 (42.8) | 2.64 | 0.94[d] | | | −1.11 |
| [**14**]$PF_6$[e] | 504 (51.4) | 2.46 | 0.93[d] | | | −0.88 |
| [**15**]$PF_6$[e] | 537 (47.5) | 2.31 | 0.96[d] | | | −0.52 |
| [**16**]$PF_6$[e] | 553 (57.2) | 2.24 | 0.95[d] | | | −0.66 |
| [**17**]$PF_6$ | 540 (43.0) | 2.30 | 0.95[d] | | | −0.84 |
| [**18**]$PF_6$[f] | 520 (61.2) | 2.38 | | | 1.01 (80) | −0.83 |
| [**19**]$PF_6$[g] | 487 (38.7) | 2.55 | 0.76[d] | | | −1.01 |
| [**20**]$PF_6$[g] | 525 (52.3) | 2.36 | 0.80[d] | | | −0.82 |
| [**21**]$PF_6$[g] | 565 (45.5) | 2.19 | 0.81[d] | | | −0.46 |
| [**22**]$PF_6$[g] | 579 (46.6) | 2.14 | 0.82[d] | | | −0.59 |
| [**23**]$PF_6$ | 560 (43.9) | 2.21 | 0.76[d] | | | −0.72 |
| [**24**]$PF_6$[f] | 558 (54.2) | 2.22 | | | 0.83 (85) | −0.69 |

[a] Solutions *ca.* $10^{-5}$ M.
[b] Solutions *ca.* $10^{-3}$ M in analyte and 0.1 M in [$N^nBu_4$]$PF_6$; potentials quoted at a scan rate of 200 mV $s^{-1}$ and using a glassy carbon working electrode for [**1**–**12**]$PF_6$ and [**17**–**24**]$PF_6$, but a platinum disc for [**13**–**16**]$PF_6$. Ferrocene internal reference $E_{1/2}$ = 0.45 V, Δ$E_p$ = 70–90 mV.
[c] $E_{pc}$ for a completely irreversible process.
[d] $E_{pa}$ for a completely irreversible process.
[e] Data taken from Ref. [8a].
[f] Data taken from Ref. [11].
[g] ICT data taken from Ref. [8c].

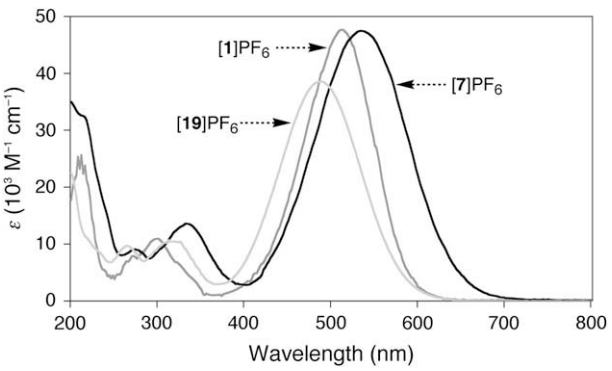


**Fig. 2.** UV–vis absorption spectra of [**1**]$PF_6$ (grey), [**7**]$PF_6$ (black) and [**19**]$PF_6$ (light grey), at 293 K in acetonitrile.

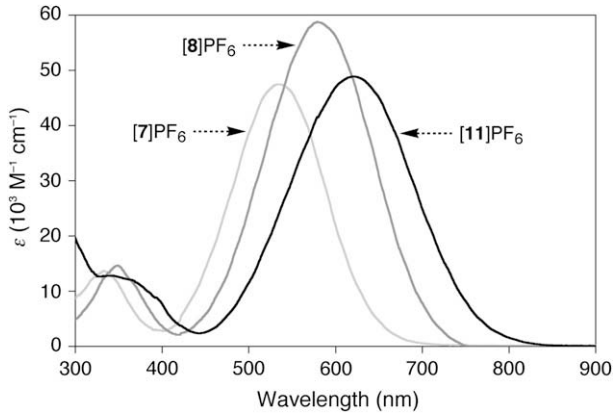


**Fig. 3.** UV–vis absorption spectra of [**7**]$PF_6$ (light grey), [**8**]$PF_6$ (grey) and [**11**]$PF_6$ (black) at 293 K in acetonitrile.

between the two extremes of *ca.* 0.4 eV. For the $n = 2$ series [**7**–**12**]$PF_6$, the ICT energies imply the electron acceptor order Mepyd < Phpyd < Mequin < Mebzt < DNPhpyd < Pympyd (Fig. 3). Essentially the same trend is observed for the Dap series [**19**–**24**]$PF_6$, but the relative positions of the Mequin and Mebzt groups are reversed, although the energy differences are only slight. The difference in $E_{max}$ between the two extremes is *ca.* 0.45 eV for [**7**–**12**]$PF_6$ and *ca.* 0.41 eV for [**19**–**24**]$PF_6$. The π-electron-accepting ability of the DNPhpyd group is diminished due to sterically induced twisting of the DNPh ring out of the plane of the chromophore [8a].

As expected, extending the bridging unit from one to two *E*-ethenyl groups causes red shifts in the ICT bands (Fig. 2), but the extent of the shifting is quite variable. For the Jd chromophores, the corresponding decreases in $E_{max}$ cover a range of *ca.* 0.08–0.22 eV, with the smallest shift for the Mequin chromophores in [**5**]$PF_6$ and [**11**]$PF_6$ and the largest for the Mebzt species in [**6**]$PF_6$ and [**12**]$PF_6$. The molar extinction coefficients $\varepsilon$ for [**1**–**12**]$PF_6$ are always somewhat larger than those of their Dap analogues (Fig. 2), but the relative difference varies considerably. $\varepsilon$ is generally not significantly influenced by *n*.

### 3.4. Electrochemistry

We have previously investigated salts [**13**–**16**]$PF_6$ by using cyclic voltammetry in acetonitrile, and observed only irreversible redox chemistry at a platinum disc working electrode [8a]. Similarly poorly defined behaviour was found for [**13**]$PF_6$ and its extended homologues such as [**19**]$PF_6$ when using a glassy carbon electrode, but under these conditions the Mebzt-containing [**18**]$PF_6$ and [**24**]$PF_6$ show fully reversible oxidation waves and completely irreversible reductive processes [11]. We have now also studied the new compounds [**1**–**12**]$PF_6$ and [**23**]$PF_6$ together with the previously reported [**17**]$PF_6$ [8f] and [**20**–**22**]$PF_6$ and the results are presented in Table 4, along with the data reported for the other compounds [8a,c,11]. Representative cyclic voltammograms of [**5**]$PF_6$ and [**17**]$PF_6$ are shown in Fig. 4.

The reduction processes in [**1**–**12**]$PF_6$ are attributed to the addition of an electron to the electron deficient pyd, Mequin or Mebzt unit; these waves generally shift to more positive potentials as the electron-accepting strength increases, although the extent of correlation with the ICT absorption energies is only partial. In particular, while the ICT data indicate that Pympyd is the strongest electron acceptor (see above), the DNPhpyd-containing compounds [**3**]$PF_6$ and [**9**]$PF_6$ have the highest $E_{pc}$ values for the reductive process. The Dap compounds show the same trend. The twisting of

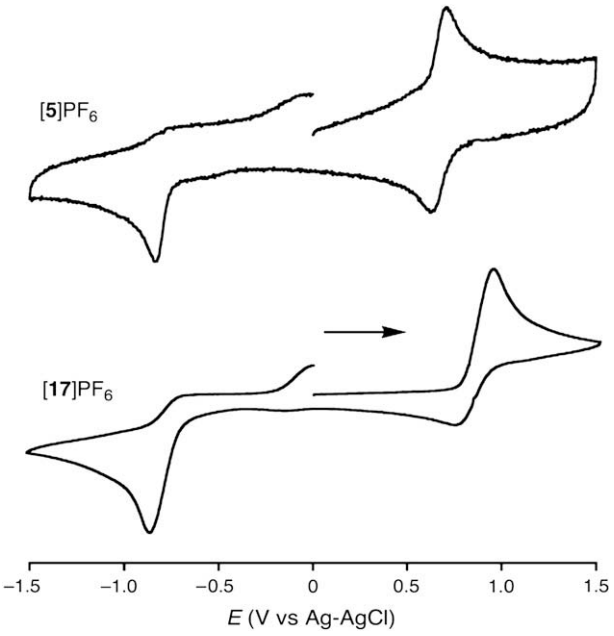


**Fig. 4.** Cyclic voltammograms of [**5**]$PF_6$ and [**17**]$PF_6$ recorded at 200 mV $s^{-1}$ in acetonitrile (the arrow indicates the direction of the initial scans).

the DNPh substituent with respect to the pyd ring (see above) probably explains this apparent discrepancy. However, given the completely irreversible nature of these processes, further speculation is unjustified. Extending the conjugated system increases $E_{pc}$ by between 60 and 180 mV; reduction occurs more readily due to stabilisation of the LUMO by greater charge delocalisation.

The oxidation processes are ascribed to the removal of an electron from the Jd/Dap-based HOMO, and the data show that the Jd unit is oxidised more readily than Dap by *ca.* 200 mV. This observation is consistent with the superior π-electron-donating strength of the Jd moiety evidenced by the $^1$H NMR and ICT absorption data (see above). For the Dap compounds, these oxidations are completely irreversible in every case, with the exception of the Mebzt derivatives [**18**]$PF_6$ and [**24**]$PF_6$, as noted previously [11]. In contrast, 5 of the 12 new Jd compounds (and mostly the $n = 1$ species) show clear return waves accompanying the oxidation wave, and in [**5**]$PF_6$, [**6**]$PF_6$ and [**12**]$PF_6$ fully reversible processes are observed. It is hence apparent that the Jd group has a greater tendency to display reversible oxidation chemistry when compared with Dap (Fig. 4); the origins of this difference in behaviour are unclear but may derive from steric effects whereby the more hindered $Jd^+$ species is less prone to engage in chemical reactions. For most of [**1**–**12**]$PF_6$, oxidation followed by reductive scanning reveals additional waves (besides those listed in Table 4) at negative potentials, that are attributable to decomposition products. This effect is especially noticeable for [**3**]$PF_6$ which shows a new peak at −1.09 V *vs* Ag–AgCl that is somewhat larger than the one at −0.57 V.

### 3.5. X-ray crystallography

This study concerns mainly molecular electronic and optical properties, but macroscopic NLO behaviour is clearly of interest for potential applications. In particular, materials that can display substantial quadratic effects must adopt favourable, polar structures. We have therefore obtained single crystal X-ray structures for the salts [**1**]$PF_6$, [**2**]$PF_6$·MeCN, [**3**–**5**]$PF_6$, [**6**]Cl·1.5MeOH, [**7**]$PF_6$, [**8**]$PF_6$, [**9**]$PF_6$, [**10**]$BPh_4$, [**11**]$PF_6$ and [**12**]$PF_6$ as well as for [**7**]Cl·

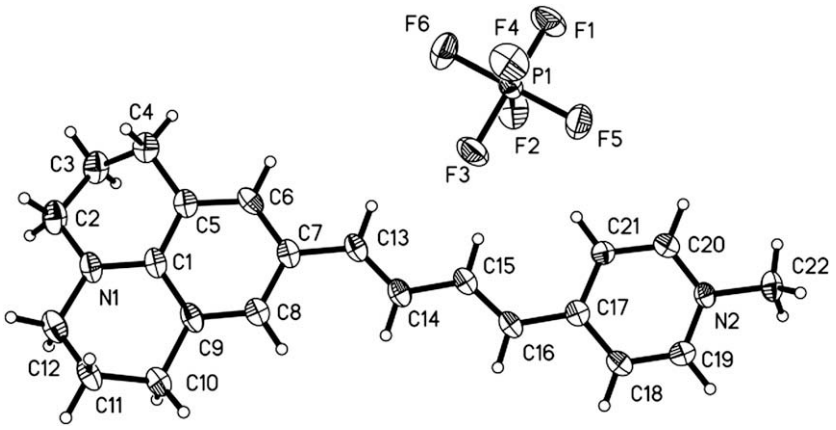


**Fig. 5.** Representation of the molecular structure of the salt [**7**]$PF_6$ (50% probability ellipsoids).

$2H_2O$ and [**7**]Cl·1.33MeOH·0.33$H_2O$ and the aldehydes Jdca and Jdpa. Representations of the molecular structures of some of the $n = 2$ $PF_6^-$ salts are shown in Figs. 5–10, and selected geometric parameters are collected in Table 5.

Several structures of Jd derivatives have been reported previously [13d,30], as well as those of a larger number of related coumarin-based compounds [31]. As expected, the Jd units in all of the compounds studied here feature essentially planar N atoms and puckered propylene chains. Of more interest is the evidence for contribution of quinoidal resonance forms to the ground-state structures, also observed in previous studies with Jd polyene chromophores [13d]. The $n = 1$ chromophores **1**–**6** show some correlation between the degree of bond length alternation (BLA) [13d,32] of the bridging ethenyl unit and the electron acceptor strength of the quaternised A group indicated by the ICT data. The structural data for the extended chromophores **7**–**12** (Table 5) permit some rather more pertinent observations because these systems are short polyenes, the class of compounds for which the BLA concept was originally derived [13d,32]. It is noteworthy that we are not aware of any other instance where structural data have been obtained for a complete series of related chromophores. Comparison with the corresponding data for **1**–**6** (BLA range = 0.260–0.058 Å) shows that the $n = 2$ chromophores have lower BLA values for every A/D combination. Furthermore, the BLA values for **7**–**12** decrease in the order A = Mepyd > Phpyd > Pympyd > Mequin > Mebzt > DNPhpyd, which is with the exception of the Pym derivative exactly the reverse of the acceptor strength ordering inferred by the ICT data (see above). This trend is entirely logical because increasing the acceptor strength with the donor kept constant should lead to greater ground-state polarization. However, the fact that the BLA values observed for the three independent cations in [**7**]Cl·1.33MeOH·0.33$H_2O$ vary by as much as 0.02 Å shows that this parameter can also be influenced significantly by crystal packing factors. Notably, the BLA of *ca*. 0.04 Å for [**9**]$PF_6$ is approximately optimised [13d], and very similar to those observed in neutral Jd-substituted polyenes [13d].

The pseudo-coplanarity of the Jd phenyl and pyd rings in most of the chromophores is consistent with significant D–A π-coupling, but unexpectedly large twists are observed in several cases. The cation in [**2**]$PF_6$·MeCN and one of the three independent cations in [**7**]Cl·1.33MeOH·0.33$H_2O$ show especially large twists of *ca*. 28°, indicating that crystal packing as well as intramolecular electronic effects also influences the molecular conformations. The pronounced twists between the pyd and DNPh rings in [**3**]$PF_6$ and [**9**]$PF_6$ arise from the steric hindrance of the ortho $-NO_2$ substituents, as observed in related structures previously [8c]. It is however noteworthy that an even larger twist is observed in [**8**]$PF_6$ which lacks such an obvious steric effect (Fig. 6). The structure of [**9**]$PF_6$ also shows a significant bowing of the *E*,*E*-1,3-butadienyl unit, but this fragment is essentially planar in all of the other structures.

Unfortunately, all of these new salts except for [**10**]$BPh_4$ adopt centrosymmetric crystal structures, precluding any significant bulk NLO effects. Although [**10**]$BPh_4$ has the space group $P2_12_12_1$, the molecular dipoles are oriented essentially antiparallel, despite the overall lack of symmetry. The aldehyde Jdca crystallises in *Cc*,

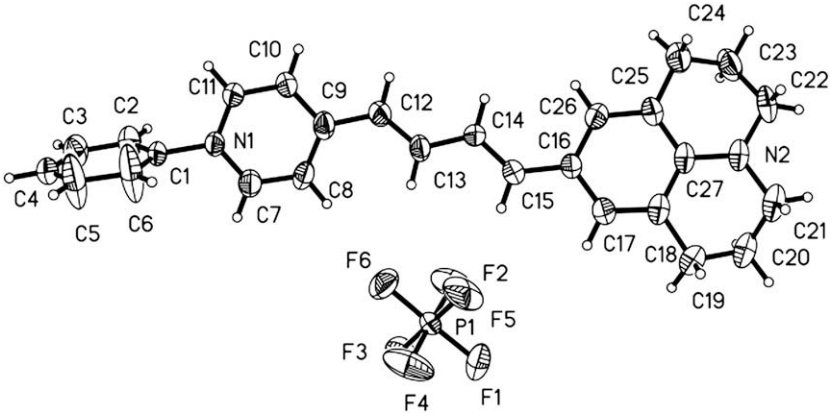


**Fig. 6.** Representation of the molecular structure of the salt [**8**]$PF_6$ (50% probability ellipsoids).

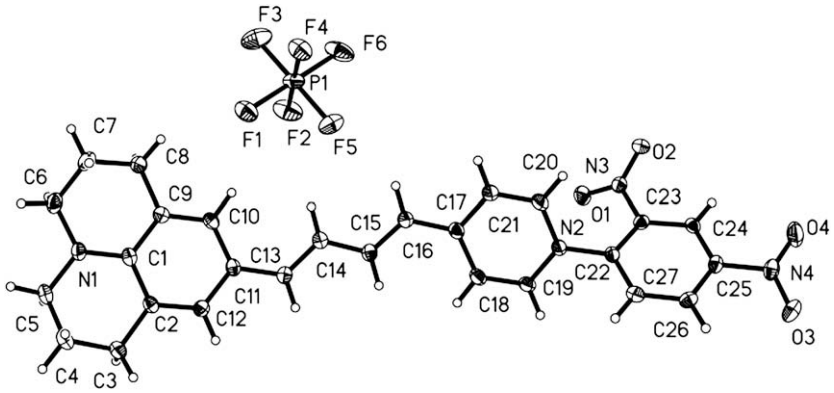


**Fig. 7.** Representation of the molecular structure of the salt [**9**]$PF_6$ (50% probability ellipsoids).

which is the same space group as that of the SHG-active form of DAST [2a,c], but again the individual dipoles cancel each other out. Comparisons with other reports [13d,30a,c–g] indicate that Jd derivatives have a clear preference for the common space groups $P\bar{1}$ and $P2_1/c$ (or the alternative setting of the same space group, $P2_1/n$). Indeed, out of a total of sixteen new structures described here, eight crystallise in $P\bar{1}$, while six adopt $P2_1/c$ or $P2_1/n$. The previous report of only modest SHG activities for the Jd analogue of DAST and several other salts of **1** [14], is consistent with our crystallographic observations. While it hence appears that the presence of the Jd moiety makes the formation of nonpolar structures even more likely than would normally be expected with chromophoric salts (for example Dap compounds), there is plenty of scope for using anion metathesis to produce further new materials that may adopt more favourable structures. It is also worth noting that various other strategies exist for arranging such charged chromophores noncentrosymmetrically, *e.g.* incorporation into polar thin films (of the Langmuir–Blodgett type) [33] and matrices such as silica zeolites or inorganic layered materials [34].

### 3.6. Hyper-Rayleigh scattering

Almost all previous studies with Jd-containing NLO chromophores have involved neutral molecules [13]. We are aware of only one related report concerning charged species in which bulk NLO measurements were carried out with the iodide, tosylate and other salts of **1**, by using the semi-quantitative Kurtz powder test for SHG [14]. Only relatively small activities were found (less than that of the urea standard when using a 1907 nm laser), but these results were attributed to unfavourable crystal packing and semi-empirical MOPAC5 calculations did predict that replacing a Dap group with Jd (*i.e.* moving from **13** to **1**) leads to an increased $\beta$ response [14]. To our knowledge, no $\beta$ measurements have been reported hitherto for charged Jd chromophores, and only the electric field-induced SHG (EFISHG) technique has been applied to neutral Jd species. The latter method requires certain other measured or predicted data in order to afford $\beta$ values, most importantly the ground-state dipole moment $\mu_g$, so it is of interest to apply other approaches. We have therefore used fs HRS experiments [24] with either a 1300 or 800 nm laser to determine $\beta$ and $\beta_0$ values (derived by using the TSM) [5] for the salts [**1**–**12**]$PF_6$ and also for [**17**]$PF_6$ and [**23**]$PF_6$ in acetonitrile. The results are shown in Table 6, together with the data reported previously for the analogous Dap compounds [**13**–**16**]$PF_6$, [**18**–**22**]$PF_6$ and [**24**]$PF_6$ [8c,11]. The data are arranged so as to facilitate comparisons between the four related series. It should be noted that the proximity of the ICT absorption to the second harmonic wavelength of 650 nm means that several of the $\beta_0$ values derived from the 1300 nm measurements are strongly underestimated and hence of limited validity.

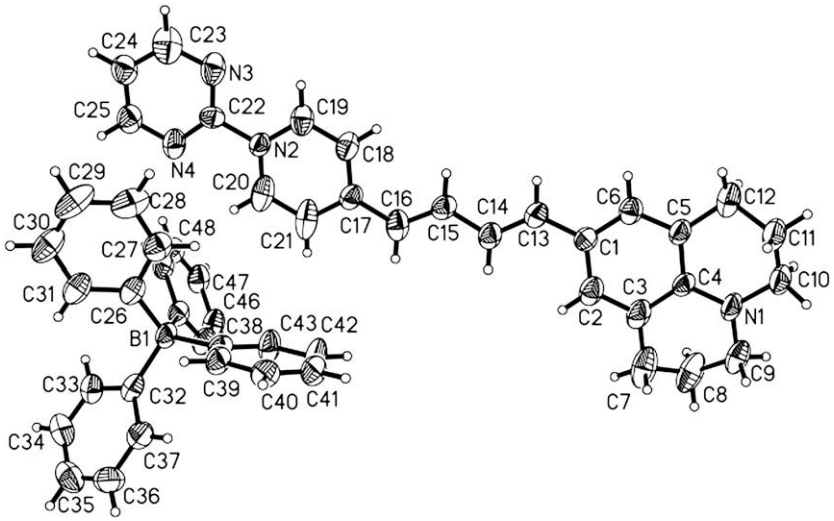


**Fig. 8.** Representation of the molecular structure of the salt [**10**]$BPh_4$ (50% probability ellipsoids).

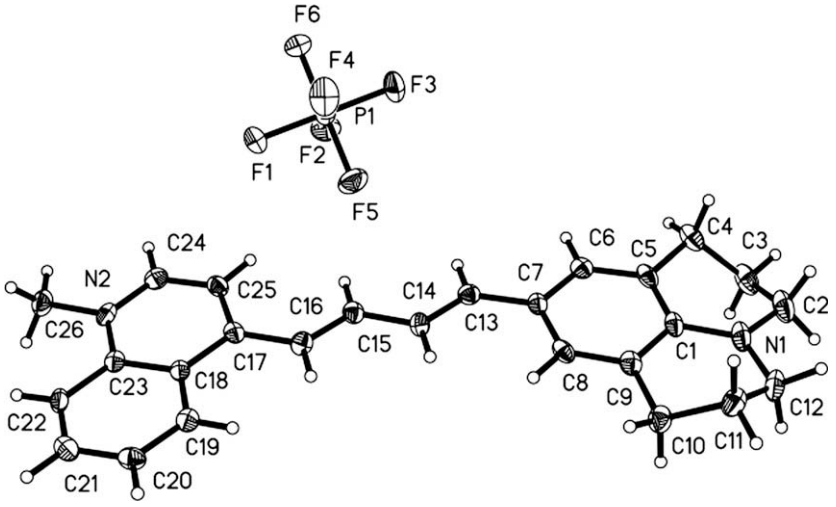


**Fig. 9.** Representation of the molecular structure of the salt [**11**]$PF_6$ (50% probability ellipsoids).

Within the $n = 1$ series [**1**–**6**]$PF_6$, the electron acceptor strength ordering deduced from the ICT energies (Mepyd < Phpyd < Mebzt < DNPhpyd ≈ Mequin < Pympyd, see above) is broadly reflected in the $\beta_0$ data, but some exceptions are evident. The $\beta_{0[800]}$ values for [**3**]$PF_6$ and [**6**]$PF_6$ are lower than expected, while the same is true of the $\beta_{0[1300]}$ data for [**4**]$PF_6$ and [**6**]$PF_6$. The observation of the largest $\beta_{0[1300]}$ response for [**2**]$PF_6$ is also clearly anomalous. It is however notable that the $\beta_0$ trends observed for [**1**–**6**]$PF_6$ are more consistent with the TSM than those for [**13**–**16**]$PF_6$ that have been discussed previously [8c]. Comparisons between the HRS data obtained for the two $n = 1$ series reveal that the superior π-electron-donating ability of the Jd group when compared with Dap that is evident in the ICT energies and other data (see above) translates into significantly larger $\beta_0$ responses in 9 out of 12 instances, with the only exceptions being the $\beta_{0[1300]}$ values for the pairs [**3**/**15**]$PF_6$, [**4**/**16**]$PF_6$ and [**5**/**17**]$PF_6$. These apparent anomalies may be due to greater underestimation of the $\beta_0$ values for the Jd species for which the $\lambda_{max}$ values are closer to the second harmonic wavelength of 650 nm when compared with their Dap analogues.

Within the extended series [**7**–**12**]$PF_6$, the ICT-deduced electron acceptor strength ordering (Mepyd < Phpyd < Mequin < Mebzt < DNPhpyd < Pympyd, see above) is almost completely opposed to the $\beta_{0[1300]}$ data, with the smallest $\beta_0$ values observed for [**9**]$PF_6$ and [**10**]$PF_6$. However, this apparent trend is a clear result of the limitations of using the simple TSM without damping corrections in cases where the ICT absorption band approaches the second harmonic wavelength. In contrast, the $\beta_{0[800]}$ values agree with the ICT trend in as much as the 2-Pym derivative [**10**]$PF_6$ has the largest response ($708 \times 10^{-30}$ esu) and this is almost twice that obtained for its Me analogue. Even so, the actual ordering within the series does not correlate well with the ICT data. The unreliability of the $\beta_{0[1300]}$ data is further evidenced by comparisons of the values for the shorter series [**1**–**6**]$PF_6$ with those of their extended homologues, since larger responses are observed for the latter in only 2 out of 6 instances. Again, the greater accuracy of the $\beta_{0[800]}$ values is borne out by the logical observation that moving from $n = 1$ to 2 causes the NLO response to increase in all cases except for the Mequin species [**5**]$PF_6$ and [**11**]$PF_6$. Similar comments can be made when comparing the HRS data obtained for the extended Jd and Dap series; the Jd chromophores have larger $\beta_{0[800]}$ values in all cases except for the Mebzt species [**12**]$PF_6$ and [**24**]$PF_6$, but the 1300 nm experiments indicate a completely opposite trend, except for the pair [**7**/**19**]$PF_6$ which have indistinguishable $\beta_{0[1300]}$ values. Given that all previous and new physical measurements confirm that the Jd group has superior π-electron-donating ability when compared with Dap, it is clear that the 800 nm HRS $\beta_0$ values are of much greater value for the compounds studied here.

### 3.7. Stark spectroscopy

We have used Stark spectroscopy in butyronitrile glasses at 77 K to afford $\Delta\mu_{12}$ values for the ICT bands of the salts [**1**–**12**]$PF_6$ and

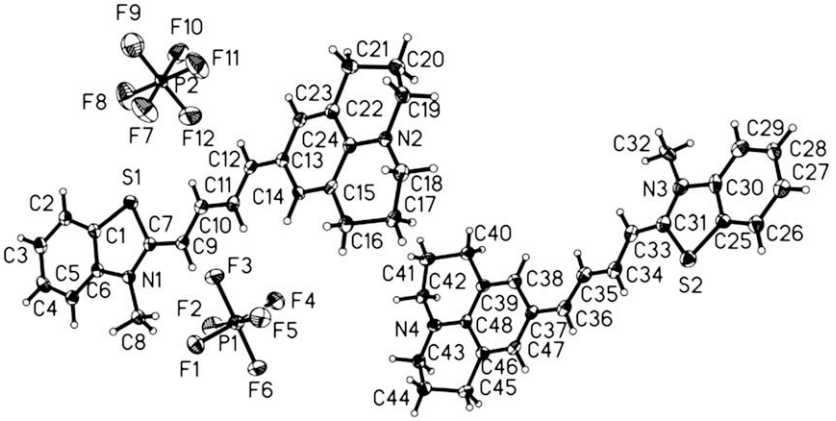


**Fig. 10.** Representation of the molecular structure of the salt [**12**]$PF_6$ (50% probability ellipsoids).

**Table 5**
Selected bond distances (Å) and dihedral angles (deg) for Jdpa and the salts [**7**]$PF_6$, [**7**]Cl·$2H_2O$, [**7**]Cl·1.33MeOH·0.33$H_2O$, [**8**]$PF_6$, [**9**]$PF_6$, [**10**]$BPh_4$, [**11**]$PF_6$ and [**12**]$PF_6$.[a]

| | Jdpa | [**7**]$PF_6$ | [**7**]Cl·$2H_2O$[b] | | [**7**]Cl·1.33MeOH·0.33$H_2O$[c] | | | [**8**]$PF_6$ | [**9**]$PF_6$ | [**10**]$BPh_4$ | [**11**]$PF_6$ | [**12**]$PF_6$[b] | |
|---|---|---|---|---|---|---|---|---|---|---|---|---|---|
| C–N(Jd) | 1.3717(14) | 1.373(3) | 1.376(4) | 1.378(4) | 1.378(4) | 1.378(4) | 1.393(4) | 1.359(4) | 1.360(2) | 1.386(6) | 1.373(2) | 1.364(4) | 1.375(4) |
| C(Ph)–C(Ph)1[d] | 1.420(2) | 1.415(4) | 1.420(7) | 1.414(6) | 1.413(7) | 1.408(7) | 1.407(6) | 1.425(6) | 1.429(4) | 1.413(10) | 1.417(3) | 1.424(7) | 1.421(7) |
| C(Ph)–C(Ph)2[e] | 1.379(2) | 1.380(4) | 1.381(6) | 1.387(7) | 1.380(6) | 1.377(6) | 1.383(6) | 1.380(6) | 1.370(4) | 1.390(10) | 1.377(3) | 1.372(7) | 1.379(7) |
| C(Ph)–C(Ph)3[f] | 1.406(2) | 1.405(4) | 1.405(7) | 1.403(6) | 1.396(7) | 1.395(7) | 1.395(6) | 1.395(6) | 1.411(4) | 1.400(10) | 1.403(3) | 1.408(7) | 1.406(7) |
| C(Ph)–C(Eth) | 1.4401(16) | 1.444(3) | 1.451(4) | 1.452(5) | 1.454(5) | 1.445(5) | 1.453(4) | 1.453(4) | 1.424(2) | 1.441(7) | 1.446(2) | 1.430(5) | 1.440(5) |
| C(Eth)–C(Eth) | 1.3495(17) | 1.337(3) | 1.342(5) | 1.348(4) | 1.340(5) | 1.353(5) | 1.336(5) | 1.348(4) | 1.372(3) | 1.354(7) | 1.348(2) | 1.360(5) | 1.360(5) |
| C(Eth)–C(Eth/C(H)CO) | 1.4389(17) | 1.430(3) | 1.433(4) | 1.433(5) | 1.431(4) | 1.430(4) | 1.435(4) | 1.419(4) | 1.405(2) | 1.431(7) | 1.418(2) | 1.400(5) | 1.413(5) |
| C(Eth)–C(Eth) | – | 1.336(3) | 1.342(5) | 1.351(4) | 1.344(5) | 1.351(5) | 1.337(5) | 1.330(4) | 1.373(3) | 1.346(7) | 1.353(2) | 1.367(5) | 1.364(5) |
| C(Eth)–C(A) | – | 1.449(3) | 1.452(4) | 1.448(5) | 1.458(5) | 1.438(5) | 1.456(5) | 1.433(4) | 1.413(3) | 1.437(7) | 1.441(2) | 1.408(5) | 1.402(5) |
| C(pyd)–C(pyd)1[g] | – | 1.396(4) | 1.402(7) | 1.403(7) | 1.392(7) | 1.405(7) | 1.399(7) | 1.395(6) | 1.422(4) | 1.386(10) | – | – | – |
| C(pyd)–C(pyd)2[h] | – | 1.368(4) | 1.365(6) | 1.368(7) | 1.368(7) | 1.370(7) | 1.371(6) | 1.362(6) | 1.352(4) | 1.369(10) | – | – | – |
| C(bzt)–N(bzt)[i] | – | – | – | – | – | – | – | – | – | – | – | 1.350(4) | 1.343(5) |
| N(A)–C(Me/Ar) | – | 1.474(3) | 1.481(4) | 1.485(4) | 1.479(4) | 1.478(4) | 1.481(4) | 1.455(3) | 1.431(2) | 1.453(6) | 1.470(2) | 1.449(4) | 1.402(4) |
| C–O | 1.2249(14) | – | – | – | – | – | – | – | – | – | – | – | – |
| Dihedral angle 1[j] | – | 6.80(7) | 5.16 | 8.22 | 2.66 | 6.12 | 27.69 | 17.72(11) | 26.28(5) | | 4.83(4) | 9.97 | 10.15 |
| Dihedral angle 1[k] | – | – | – | – | – | – | – | 82.72(13) | 54.84(6) | | – | – | – |
| BLA[l] | – | 0.104 | 0.103 | 0.094 | 0.106 | 0.086 | 0.111 | 0.096 | 0.041 | 0.086 | 0.084 | 0.049 | 0.056 |

[a] Eth = ethenyl.
[b] For the two independent cations.
[c] For the three independent cations.
[d] Average C(N)–C(C) distance in Jd phenyl ring.
[e] Average C($CH_2$)–CH distance in Jd phenyl ring.
[f] Average CH–C(CH) distance in Jd phenyl ring.
[g] Average C(C)–CH distance in pyd ring.
[h] Average CH–CH distance in pyd ring.
[i] Distance to methylated N atom.
[j] Between planes of Jd phenyl and pyd rings.
[k] Between planes of pyd and *N*-aryl rings.
[l] Bond length alternation for the *E*,*E*-1,3-butadienyl bridge, defined as the difference between the average C–C and C=C distances [13d].

[**23**]$PF_6$. Selected data are shown in Table 7, together with those for [**13**–**21**]$PF_6$ and [**24**]$PF_6$ which we have reported previously (unfortunately, a satisfactory data fit could not be obtained for [**22**]$PF_6$) [8c,f,11]. Again, these data are arranged to facilitate comparisons between the three related series. As with the previously studied Mebzt compounds including [**18**]$PF_6$ and [**24**]$PF_6$ [11], the ICT absorption spectra of [**6**]$PF_6$ and [**12**]$PF_6$ change from being single apparently symmetrical bands at 293 K in acetonitrile solutions to having structured profiles at 77 K in a butyronitrile glass. The data for these compounds were hence treated by using Gaussian deconvolution with two curves, the first and second derivatives of which were used to fit the Stark spectrum.

In most cases, the ICT bands of [**1**–**12**]$PF_6$ show small red shifts on moving from acetonitrile solutions to butyronitrile glasses, and the energy ordering within the two series remains unchanged (Tables 4 and 7). However, the difference in $E_{max}$ between [**3**]$PF_6$ and [**5**]$PF_6$ increases from 0.01 to 0.05 eV in the frozen medium. The decreases in $E_{max}$ on moving from [**1**–**6**]$PF_6$ to their extended analogues are also maintained at 77 K, and cover a range of *ca.* 0.09–0.21 eV, in similar fashion to the room temperature spectra. Also, replacing the Dap group with Jd always decreases $E_{max}$, irrespective of the conditions. The $f_{os}$, $\mu_{12}$ and $c_b^2$ values for [**1**–**12**]$PF_6$ generally increase with acceptor strength, but no clear trends are observed for the parameters $\Delta\mu_{12}$, $\Delta\mu_{ab}$, $r_{12}$, $r_{ab}$, or $H_{ab}$. Extension of the conjugation on moving from [**1**–**6**]$PF_6$ to [**7**–**12**]$PF_6$ causes increases in $f_{os}$, $\mu_{12}$, $\Delta\mu_{12}$, $\Delta\mu_{ab}$, $r_{12}$ and $r_{ab}$, while corresponding decreases are found for $c_b^2$ and $H_{ab}$. These observations are all consistent with expectations; dipole moment changes and electron-transfer distances increase with chromophore length whereas D–A electronic coupling (and orbital mixing) becomes weaker over longer distances.

Because the chromophores in [**1**–**12**]$PF_6$ and [**23**]$PF_6$ are essentially linear dipoles, it is reasonable to use the standard TSM [5] to estimate $\beta_0$ values from the Stark data (as with the HRS data, see above). With the clear exception of [**6**]$PF_6$, the values of $\beta_0$

**Table 6**
ICT absorption and HRS data for the salts [**1**–**24**]$PF_6$ in acetonitrile.

| salt | $\lambda_{max}$ (nm) | $\beta_{1300}$[a] ($10^{-30}$ esu) | $\beta_{0[1300]}$[b] ($10^{-30}$ esu) | $\beta_{800}$[c] ($10^{-30}$ esu) | $\beta_{0[800]}$[d] ($10^{-30}$ esu) |
|---|---|---|---|---|---|
| [**1**]$PF_6$ | 515 | 241 ± 16 | 76 ± 5 | 573 ± 45 | 220 ± 17 |
| [**7**]$PF_6$ | 533 | 1055 ± 140 | 288 ± 38 | 878 ± 34 | 379 ± 15 |
| [**13**]$PF_6$[e] | 470 | 55 ± 10 | 25 ± 4 | 440 ± 30 | 110 ± 7 |
| [**19**]$PF_6$[e] | 488 | 770 ± 270 | 290 ± 100 | 166 ± 20 | 51 ± 6 |
| [**2**]$PF_6$ | 556 | 1166 ± 59 | 256 ± 13 | 629 ± 26 | 303 ± 13 |
| [**8**]$PF_6$ | 579 | 1373 ± 237 | 227 ± 39 | 839 ± 59 | 438 ± 31 |
| [**14**]$PF_6$[e] | 504 | 405 ± 40 | 120 ± 12 | 290 ± 20 | 102 ± 7 |
| [**20**]$PF_6$[e] | 524 | 1500 ± 220 | 445 ± 65 | 301 ± 20 | 123 ± 8 |
| [**3**]$PF_6$ | 595 | 822 ± 40 | 105 ± 5 | 312 ± 26 | 169 ± 14 |
| [**9**]$PF_6$ | 639 | 1500 ± 157 | 38 ± 4[f] | 744 ± 94 | 418 ± 53 |
| [**15**]$PF_6$[e] | 536 | 370 ± 35 | 100 ± 9 | 295 ± 20 | 130 ± 9 |
| [**21**]$PF_6$[e] | 568 | 1200 ± 45 | 230 ± 9 | 304 ± 32 | 153 ± 16 |
| [**4**]$PF_6$ | 615 | 1505 ± 48 | 122 ± 4 | 898 ± 23 | 501 ± 13 |
| [**10**]$PF_6$ | 662 | 1454 ± 68 | 40 ± 2[f] | 1292 ± 81 | 708 ± 44 |
| [**16**]$PF_6$[e] | 553 | 1130 ± 20 | 230 ± 4 | 270 ± 20 | 130 ± 9 |
| [**22**]$PF_6$[e] | 578 | 1370 ± 22 | 230 ± 4 | 435 ± 50 | 226 ± 26 |
| [**5**]$PF_6$ | 596 | 1092 ± 31 | 137 ± 4 | 898 ± 11 | 487 ± 6 |
| [**11**]$PF_6$ | 621 | 1156 ± 219 | 79 ± 15 | 479 ± 37 | 269 ± 21 |
| [**17**]$PF_6$ | 540 | 627 ± 43 | 161 ± 11 | 570 ± 24 | 255 ± 11 |
| [**23**]$PF_6$ | 560 | 2546 ± 170 | 534 ± 36 | 438 ± 18 | 214 ± 9 |
| [**6**]$PF_6$ | 564 | 339 ± 19 | 68 ± 4 | 477 ± 16 | 237 ± 8 |
| [**12**]$PF_6$ | 631 | 2130 ± 76 | 94 ± 3[f] | 650 ± 36 | 366 ± 20 |
| [**18**]$PF_6$[g] | 520 | —[h] | | 425 ± 15 | 170 ± 6 |
| [**24**]$PF_6$[g] | 558 | 5400 ± 500 | 1160 ± 110 | 1040 ± 35 | 510 ± 17 |

[a] Measured using a 1300 nm laser.
[b] Estimated from $\beta_{1300}$ via the TSM [5].
[c] Measured using an 800 nm laser.
[d] Estimated from $\beta_{800}$ via the TSM [5]. The quoted cgs units (esu) can be converted into SI units ($C^3\,m^3\,J^{-2}$) by dividing by a factor of $2.693 \times 10^{20}$.
[e] Data taken from Ref. [8b].
[f] Heavily underestimated due to resonance enhancement.
[g] Data taken from Ref. [11].
[h] No signal observed.

**Table 7**
Selected visible absorption, Stark spectroscopic and derived data for salts [**1**–**21**]$PF_6$, [**23**]$PF_6$ and [**24**]$PF_6$.[a]

| salt | $\lambda_{max}$ (nm) | $E_{max}$ (eV) | $f_{os}$ | $\mu_{12}$[b] (D) | $\Delta\mu_{12}$[c] (D) | $\Delta\mu_{ab}$[d] (D) | $r_{12}$[e] (Å) | $r_{ab}$[f] (Å) | $c_b^2$[g] | $H_{ab}$[h] ($10^3$ $cm^{-1}$) | $\beta_0$[S][i] ($10^{-30}$ esu) |
|---|---|---|---|---|---|---|---|---|---|---|---|
| [**1**]$PF_6$ | 518 | 2.39 | 0.55 | 7.8 | 17.9 | 23.8 | 3.7 | 5.0 | 0.12 | 6.4 | 214 |
| [**7**]$PF_6$ | 541 | 2.29 | 0.76 | 10.1 | 25.6 | 31.8 | 5.3 | 6.6 | 0.10 | 5.5 | 497 |
| [**13**]$PF_6$[j] | 480 | 2.58 | 0.80 | 9.1 | 16.3 | 24.4 | 3.4 | 5.1 | 0.17 | 7.7 | 236 |
| [**19**]$PF_6$[j] | 503 | 2.47 | 0.78 | 9.1 | 20.4 | 27.4 | 4.2 | 5.7 | 0.13 | 6.6 | 328 |
| [**2**]$PF_6$ | 559 | 2.22 | 0.78 | 9.6 | 17.3 | 25.9 | 3.6 | 5.4 | 0.17 | 6.7 | 376 |
| [**8**]$PF_6$ | 588 | 2.11 | 0.93 | 10.8 | 22.8 | 31.4 | 4.7 | 6.5 | 0.14 | 6.0 | 702 |
| [**14**]$PF_6$[j] | 514 | 2.41 | 0.80 | 9.4 | 16.3 | 24.8 | 3.4 | 5.2 | 0.17 | 7.3 | 288 |
| [**20**]$PF_6$[j] | 546 | 2.27 | 1.24 | 12.0 | 19.1 | 30.6 | 4.0 | 6.4 | 0.19 | 7.2 | 622 |
| [**3**]$PF_6$ | 588 | 2.11 | 0.80 | 10.0 | 18.8 | 27.5 | 3.9 | 5.7 | 0.16 | 6.2 | 468 |
| [**9**]$PF_6$ | 633 | 1.96 | 0.91 | 11.0 | 23.9 | 32.5 | 5.0 | 6.8 | 0.14 | 5.4 | 879 |
| [**15**]$PF_6$[j] | 537 | 2.31 | 0.78 | 9.5 | 18.4 | 26.4 | 3.8 | 5.5 | 0.15 | 6.7 | 362 |
| [**21**]$PF_6$[j] | 574 | 2.16 | 0.88 | 10.4 | 26.0 | 33.3 | 5.4 | 6.9 | 0.11 | 5.5 | 706 |
| [**4**]$PF_6$ | 617 | 2.01 | 0.86 | 10.7 | 16.9 | 27.2 | 3.5 | 5.7 | 0.19 | 6.4 | 544 |
| [**10**]$PF_6$ | 658 | 1.88 | 1.06 | 12.2 | 22.0 | 32.8 | 4.6 | 6.8 | 0.16 | 5.7 | 1050 |
| [**16**]$PF_6$[j] | 563 | 2.20 | 0.76 | 9.5 | 14.5 | 23.9 | 3.0 | 5.0 | 0.20 | 7.1 | 318 |
| [**5**]$PF_6$ | 602 | 2.06 | 0.68 | 9.4 | 17.5 | 25.6 | 3.6 | 5.3 | 0.16 | 6.1 | 444 |
| [**11**]$PF_6$ | 629 | 1.97 | 0.81 | 10.5 | 22.6 | 30.8 | 4.7 | 6.4 | 0.16 | 5.4 | 745 |
| [**17**]$PF_6$[k] | 553 | 2.24 | 0.70 | 9.1 | 13.3 | 22.5 | 2.8 | 4.7 | 0.21 | 7.3 | 255 |
| [**23**]$PF_6$ | 582 | 2.13 | 0.95 | 10.9 | 19.4 | 29.2 | 4.0 | 6.1 | 0.17 | 6.4 | 590 |
| [**6**]$PF_6$[l] | 568 | 2.18 | 0.86 | 10.2 | 7.6 | 21.8 | 1.6 | 4.5 | 0.33 | 8.3 | 178 |
| | 571 | 2.17 | 0.34 | 6.4 | 7.3 | 14.9 | 1.5 | 3.1 | 0.25 | 7.6 | 76 |
| | 538 | 2.31 | 0.49 | 7.5 | 8.3 | 17.1 | 1.7 | 3.6 | 0.26 | 8.1 | 99 |
| [**12**]$PF_6$[l] | 629 | 1.97 | 0.89 | 10.9 | 14.8 | 26.4 | 3.1 | 5.5 | 0.22 | 6.6 | 528 |
| | 637 | 1.95 | 0.25 | 5.7 | 13.1 | 17.4 | 2.7 | 3.6 | 0.13 | 5.2 | 133 |
| | 592 | 2.10 | 0.60 | 8.7 | 17.3 | 22.9 | 3.6 | 4.8 | 0.18 | 6.4 | 298 |
| [**18**]$PF_6$[m] | 532 | 2.33 | 0.35 | 6.3 | 8.1 | 14.9 | 1.7 | 3.1 | 0.23 | 7.9 | 68 |
| | 495 | 2.50 | 0.30 | 5.7 | 5.3 | 12.5 | 1.1 | 2.6 | 0.29 | 9.1 | 32 |
| | 489 | 2.54 | 0.59 | 7.6 | 16.3 | 22.6 | 3.4 | 4.7 | 0.14 | 7.1 | 182 |
| [**24**]$PF_6$[m] | 590 | 2.10 | 0.28 | 5.9 | 11.2 | 16.3 | 2.3 | 3.4 | 0.16 | 6.2 | 104 |
| | 550 | 2.25 | 0.28 | 5.7 | 11.1 | 15.9 | 2.3 | 3.3 | 0.15 | 6.5 | 83 |
| | 531 | 2.34 | 0.63 | 8.5 | 15.3 | 22.8 | 3.2 | 4.8 | 0.16 | 7.0 | 234 |

[a] In butyronitrile glasses at 77 K.
[b] Derived from Eq. (2).
[c] Calculated from $f_{int}\Delta\mu_{12}$ using $f_{int} = 1.33$.
[d] Calculated from Eq. (1).
[e] Delocalised electron-transfer distance calculated from $\Delta\mu_{12}/e$.
[f] Effective (localised) electron-transfer distance calculated from $\Delta\mu_{ab}/e$.
[g] Calculated from Eq. (3).
[h] Calculated from Eq. (4).
[i] Calculated from Eq. (5).
[j] Data taken from Ref. [8c].
[k] Data taken in part from Ref. [8f].
[l] First line of data obtained without any spectral deconvolution; second and third lines correspond with data obtained by using two Gaussian functions.
[m] Data taken from Ref. [11] and fitted by using three Gaussian functions.

calculated via Eq. (5) for the $n = 1$ species show an expected steady increase with acceptor strength, with the results for [**3**]$PF_6$ and [**5**]$PF_6$ being indistinguishable. On moving along the pyd series [**1**–**4**]$PF_6$, a *ca.* 2.5-fold increase in $\beta_0$ is predicted. Except for the Mebzt-based [**12**]$PF_6$, the $\beta_0$ values calculated for the $n = 2$ chromophores also increase steadily with acceptor strength, with a *ca.* 2-fold enhancement along the series [**7**–**10**]$PF_6$. Again in accord with expectations, the NLO responses of [**7**–**12**]$PF_6$ are considerably larger than those of their shorter homologues; the relative difference is about 2-fold in all cases except for [**6**]$PF_6$ and [**12**]$PF_6$, which show a *ca.* 3-fold $\beta_0$ increase when considering only the data obtained without Gaussian deconvolution. These increased NLO responses arise from the combined effects of decreasing $E_{max}$ and increasing $\mu_{12}$ and $\Delta\mu_{12}$. The $\beta_0$ value of *ca.* $10^{-27}$ esu determined for [**10**]$PF_6$ is especially large for a relatively small organic chromophore.

Excluding the Mebzt compounds, comparisons between the Jd/Dap pairs reveal no clear trends in $f_{os}$ or $\mu_{12}$, but the values of $\Delta\mu_{12}$, $\Delta\mu_{ab}$, $r_{12}$ and $r_{ab}$ are generally slightly larger for the Jd species (Table 7). In contrast, the latter mostly show smaller values of $c_b^2$ and $H_{ab}$. In 7 out of 9 cases, replacing Dap with Jd increases $\beta_0$ significantly, with a relative increase of as much as *ca.* 75% on moving from [**17**]$PF_6$ to [**5**]$PF_6$. The only pair for which a corresponding decrease is observed ([**1**]$PF_6$ and [**13**]$PF_6$) have similar values. These enhancements in NLO response are due to the markedly decreased $E_{max}$ values and slightly larger $\Delta\mu_{12}$ values of the Jd chromophores.

The new results for the Mebzt compounds [**6**]$PF_6$ and [**12**]$PF_6$ allow comparisons between the analyses with and without Gaussian deconvolution. For [**6**]$PF_6$, the $\beta_0$ value is essentially the same when using either approach ($175–178 \times 10^{-30}$ esu), while a somewhat smaller value is derived for [**12**]$PF_6$ when summing the two components (431 *vs* $528 \times 10^{-30}$ esu). Notably, applying deconvolution to the ICT spectra for [**7**–**11**]$PF_6$ in all cases affords total $\beta_0$ values that are very similar to those determined without using spectral fitting (Table 7). Considering the total $\beta_0$ responses, a decrease is observed on moving from [**18**]$PF_6$ to [**6**]$PF_6$, while no significant difference is apparent between [**24**]$PF_6$ and [**12**]$PF_6$. These results therefore contradict the general trend of increasing NLO response upon replacing Dap with Jd, although the data for [**6**]$PF_6$, [**12**]$PF_6$, [**18**]$PF_6$ and [**24**]$PF_6$ may be less reliable due to the added uncertainties introduced by deconvolution. However, the HRS results for these Mebzt species also show conflicting behaviour, with $\beta_{0[800]}$ increasing on moving from [**18**]$PF_6$ to [**6**]$PF_6$, but decreasing going from [**24**]$PF_6$ to [**12**]$PF_6$ (Table 6).

Taken as a whole, our Stark results confirm that replacing the Dap donor with Jd in charged chromophores usually leads to

substantially enhanced $\beta_0$ responses, consistent with the increased electron-donating ability of the Jd group indicated by the ICT absorption and other measurements and also verified by most of the HRS experiments (see above). The 800 nm HRS data indicate that the relative increase in $\beta_0$ on replacing Dap with Jd is *ca.* 25–645%, while the Stark results give a corresponding range of *ca.* 15–75%. This general conclusion is also consistent with the results of most previous EFISHG measurements made with pairs of Dap/Jd-containing neutral chromophores [13c–e], although it should be noted that in at least two instances a reverse trend has been observed [13a,c]. These reported anomalies whereby a Dap derivative shows a larger $\beta_0$ response when compared with its Jd analogue cannot be explained by invoking BLA or resonance considerations. However, according to EFISHG, relative increases in $\beta_0$ of *ca.* 20–50% generally occur on replacing Dap with Jd, with most being nearer to 20% [13c,d]. Qualitatively, the increased electron-donating effect of the Jd moiety has been attributed to the combined effects of the alkyl units and the enforced planarity of the N atom [14]. Although our results largely confirm expectations, the observed $\beta_0$ increases are mostly somewhat greater (and in some cases much greater) than those expected when compared with previous EFISHG studies. In addition, our range of comparative and inter-related physical data is unprecedented and helps to explain quantitatively the origins of the superior donor ability of the Jd group.

Given the technological importance of DAST, it is worth highlighting how the NLO responses of our new chromophores compare with the cation **13**. For example, the respective $\beta_0$ values determined for [**10**]$PF_6$ using 800 nm HRS and Stark data of 708 and $1050 \times 10^{-30}$ esu are increased by about 4- to 6-fold when compared with the corresponding results (110 and $236 \times 10^{-30}$ esu) for **13** [8c]. These observations provide a strong incentive to pursue polar materials incorporating our new cations, in which exceptionally large bulk NLO effects may be anticipated.

## 4. Conclusions

We have synthesised and characterised a large series of salts of cationic chromophores with electron-donating Jd groups, in part to allow comparisons with related Dap species that have been studied more intensively. ICT absorption spectra show that replacing Dap with Jd leads to substantial red shifts, due to the superior π-electron-donating ability of the latter. These observations are corroborated by $^1$H NMR chemical shifts and also by cyclic voltammetry which shows that the Jd unit is oxidised more readily than Dap. The $\beta_0$ values determined via HRS measurements in acetonitrile at 650 nm are generally of little use due to extensive resonance enhancement and the limitations of the undamped TSM approximation. In contrast, the HRS data derived from experiments using an 800 nm laser are much more informative and agree reasonably well with the $\beta_0$ responses deduced from Stark spectroscopy at 77 K in butyronitrile glasses. Although some exceptions are evident, most of the data show that the use of Jd in place of Dap is an effective strategy for enhancing $\beta_0$ responses, giving several-fold increases in some cases. Single crystal X-ray structures have been determined for fourteen salts; the adoption of centrosymmetric packing arrangements in all but one case shows that the Jd moiety has an unfortunate tendency to favour such structures, at least with $PF_6^-$ or $Cl^-$ counter-anions. The one noncentrosymmetric material (a $BPh_4^-$ salt) nevertheless features antiparallel molecular dipoles. Although a limited statistical analysis of crystallographic data for neutral compounds indicates that dipole–dipole interactions (using AMPAC-computed $\mu_g$ values) do not influence solid state organisation[35], it appears plausible that the unusually strong tendency for dipole cancellation in our compounds may be connected with their high $\mu_g$ values associated with the presence of the strong Jd donor group. Notably, the structural data for the salts of extended chromophores provide an unusual complete series in which the observed BLA generally correlates with the increasing electron acceptor strength, with one chromophore showing an optimum value of *ca.* 0.04 Å. We have achieved $\beta_0$ values as large as *ca.* $10^{-27}$ esu, about 6 times that of the chromophore in the technologically important material DAST. Therefore, anion metathesis or other more controlled approaches to achieve dipolar alignment may be expected to produce further new materials that display very pronounced bulk NLO behaviour.

## Acknowledgements

We thank the EPSRC for support (grants GR/M93864 and EP/D070732 and a PhD studentship to ECH) and also the Fund for Scientific Research-Flanders (FWO-V, G.0312.08) and the University of Leuven (GOA/2006/3). We thank Dr. John E. Warren (Synchrotron Radiation Source, CCLRC, Daresbury Laboratory, Warrington, WA4 4AD, UK) for assistance with the crystal structure determination of compound [**10**]$BPh_4$.

## References

[1] (a) Chemla DS, Zyss J, editors. Nonlinear optical properties of organic molecules and crystals, vols. 1 and 2. Orlando, FL: Academic Press; 1987;
(b) Zyss J, editor. Molecular nonlinear optics: materials, physics and devices. Boston: Academic Press; 1994;
(c) Bosshard Ch, Sutter K, Prêtre Ph, Hulliger J, Flörsheimer M, Kaatz P, Günter P, editors. Organic nonlinear optical materials (advances in nonlinear optics), vol. 1. Amsterdam, The Netherlands: Gordon & Breach; 1995;
(d) Nalwa HS, Miyata S, editors. Nonlinear optics of organic molecules and polymers. Boca Raton, FL: CRC Press; 1997;
(e) Papadopoulos MG, Leszczynski J, Sadlej AJ, editors. Nonlinear optical properties of matter: from molecules to condensed phases. Dordrecht: Springer; 2006.

[2] Selected examples: (a) Marder SR, Perry JW, Schaefer WP. Science 1989;245:626–8;
(b) Marder SR, Perry JW, Schaefer WP. J Mater Chem 1992;2:985–6;
(c) Marder SR, Perry JW, Yakymyshyn CP. Chem Mater 1994;6:1137–47;
(d) Lee O-K, Kim K-S. Photonics Sci News 1999;4:9–20;
(e) Sohma S, Takahashi H, Taniuchi T, Ito H. Chem Phys 1999;245:359–64;
(f) Kaino T, Cai B, Takayama K. Adv Funct Mater 2002;12:599–603;
(g) Mohan Kumar R, Rajan Babu D, Ravi G, Jayavel R. J Cryst Growth 2003;250:113–7;
(h) Geis W, Sinta R, Mowers W, Deneault SJ, Marchant MF, Krohn KE, et al. Appl Phys Lett 2004;84:3729–31.

[3] Selected examples: (a) Yitzchaik S, Marks TJ. Acc Chem Res 1996;29:197–202;
(b) Alain V, Blanchard-Desce M, Ledoux-Rak I, Zyss J. Chem Commun 2000:353–4;
(c) Cariati E, Ugo R, Cariati F, Roberto D, Masciocchi N, Galli S, et al. Adv Mater 2001;13:1665–8;
(d) Abbotto A, Beverina L, Bradamante S, Facchetti A, Klein C, Pagani GA, et al. Chem–Eur J 2003;9:1991–2007;
(e) Kim HS, Lee SM, Ha K, Jung C, Lee Y-J, Chun YS, et al. J Am Chem Soc 2004;126:673–82;
(f) Yang Z, Aravazhi S, Schneider A, Seiler P, Jazbinšek M, Günter P. Adv Funct Mater 2005;15:1072–6;
(g) Ruiz B, Yang Z, Gramlich V, Jazbinšek M, Günter P. J Mater Chem 2006;16:2839–42;
(h) Kim HS, Sohn KW, Jeon Y, Min H, Kim D, Yoon KB. Adv Mater 2007;19:260–3;
(i) Yang Z, Jazbinšek M, Ruiz B, Aravazhi S, Gramlich V, Günter P. Chem Mater 2007;19:3512–8.

[4] Examples: (a) Kawase K, Mizuno M, Sohma S, Takahashi H, Taniuchi T, Urata Y, et al. Opt Lett 1999;24:1065–7;
(b) Kawase K, Hatanaka T, Takahashi H, Nakamura K, Taniuchi T, Ito H. Opt Lett 2000;25:1714–6;
(c) Taniuchi T, Okada S, Nakanishi H. Appl Phys Lett 2004;95:5984–8;
(d) Taniuchi T, Ikeda S, Okada S, Nakanishi H. Jap J Appl Phys 2005;44:L652–4;
(e) Schneider A, Neis M, Stillhart M, Ruiz B, Khan RUA, Günter P. J Opt Soc Am B 2006;23:1822–35;
(f) Schneider A, Stillhart M, Günter P. Opt Express 2006;14:5376–84;
(g) Yang Z, Mutter L, Stillhart M, Ruiz B, Aravazhi S, Jazbinšek M, et al. Adv Funct Mater 2007;17:2018–23.

[5] (a) Oudar JL, Chemla DS. J Chem Phys 1977;66:2664–8;
(b) Oudar JL. J Chem Phys 1977;67:446–57.

[6] (a) Clays K, Persoons A. Phys Rev Lett 1991;66:2980–3;
(b) Hendrickx E, Clays K, Persoons A. Acc Chem Res 1998;31:675–83.
[7] (a) Liptay W. In: Lim EC, editor. Excited states, vol. 1. New York: Academic Press; 1974. p. 129–229;
(b) Bublitz GU, Boxer SG. Annu Rev Phys Chem 1997;48:213–42.
[8] (a) Coe BJ, Harris JA, Asselberghs I, Clays K, Olbrechts G, Persoons A, et al. Adv Funct Mater 2002;12:110–6;
(b) Clays K, Coe BJ. Chem Mater 2003;15:642–8;
(c) Coe BJ, Harris JA, Asselberghs I, Wostyn K, Clays K, Persoons A, et al. Adv Funct Mater 2003;13:347–57;
(d) Coe BJ, Harris JA, Brunschwig BS, Garín J, Orduna J, Coles SJ, et al. J Am Chem Soc 2004;126:10418–27;
(e) Coe BJ, Beljonne D, Vogel H, Garín J, Orduna J. J Phys Chem A 2005;109:10052–7;
(f) Coe BJ, Hall JJ, Harris JA, Brunschwig BS, Coles SJ, Hursthouse MB. Acta Crystallogr Sect E 2005;61:o464–7.
[9] Ruiz B, Coe BJ, Gianotti R, Gramlich V, Jazbinšek M, Günter P. CrystEngComm 2007;9:772–6.
[10] Figi H, Mutter L, Hunziker C, Jazbinšek M, Günter P, Coe BJ. J Opt Soc Am B 2008;25:1786–93.
[11] Coe BJ, Harris JA, Hall JJ, Brunschwig BS, Hung S-T, Libaers W, et al. Chem Mater 2006;18:5907–18.
[12] Coe BJ, Harris JA, Brunschwig BS, Garín J, Orduna J. J Am Chem Soc 2005;127:3284–5.
[13] Selected examples: (a) Singer KD, Sohn JE, King LA, Gordon HM, Katz HE, Dirk CW. J Opt Soc Am B 1989;6:1339–48;
(b) Hayden LM, Sauter GF, Ore FR, Pasillas PL, Hoover JM, Lindsay GA, et al. J Appl Phys 1990;68:456–65;
(c) Cheng L-T, Tam W, Stevenson SH, Meredith GR, Rikken G, Marder SR. J Phys Chem 1991;95:10631–43;
(d) Marder SR, Cheng L-T, Tiemann BG, Friedli AC, Blanchard-Desce M, Perry JW, et al. Science 1994;263:511–4;
(e) Moylan CR. J Phys Chem 1994;98:13513–6;
(f) Lu D, Marten B, Cao Y-X, Ringnalda MN, Friesner RA, Goddard III WA. Chem Phys Lett 1995;242:543–7;
(g) Blanchard-Desce M, Alain V, Bedworth PV, Marder SR, Fort A, Runser C, et al. Chem–Eur J 1997;3:1091–104;
(h) Alain V, Thouin L, Blanchard-Desce M, Gubler U, Bosshard C, Günter P, et al. Adv Mater 1999;11:1210–4;
(i) Dai T, Singer KD, Twieg RJ, Kowalczyk TC. J Opt Soc Am B 2000;17:412–21;
(j) Myers Kelley A. J Opt Soc Am B 2002;19:1890–900;
(k) Isborn CM, Leclercq A, Vila FD, Dalton LR, Brédas JL, Eichinger BE, et al. J Phys Chem A 2007;111:1319–27.
[14] Bruce DW, Denning RG, Grayson M, Le Lagadec R, Lai KK, Pickup BT, et al. Adv Mater Opt Electron 1994;4:293–301.
[15] Murrill P. J Am Chem Soc 1899;21:828–54.
[16] Buffa R, Zahradnik P, Foltinova P. Heterocyclic Commun 2001;7:331–6.
[17] Haidekker MA, Ling T, Anglo M, Stevens HY, Frangos JA, Theodorakis EA. Chem Biol 2001;8:123–31.
[18] SAINT (Version 6.45) and SADABS (Version 2.10). Madison, Wisconsin, USA: Bruker AXS Inc; 2003.
[19] Sheldrick GM. Acta Crystallogr Sect A 1990;46:467–73.
[20] Sheldrick GM. SHELXL 97, Program for crystal structure refinement. Göttingen, Germany: University of Göttingen; 1997.
[21] SHELXTL (Version 6.10). Madison: Wisconsin, USA: Bruker AXS Inc; 2000.
[22] Sheldrick GM. TWINABS. Germany: University of Göttingen; 2007.
[23] Sheldrick GM. CELL_NOW. Germany: University of Göttingen; 2005.
[24] (a) Olbrechts G, Strobbe R, Clays K, Persoons A. Rev Sci Instrum 1998;69:2233–41. (b) Olbrechts G, Wostyn K, Clays K, Persoons A. Optics Lett 1999;24:403–5;
(c) Clays K, Wostyn K, Olbrechts G, Persoons A, Watanabe A, Nogi K, et al. J Opt Soc Am B 2000;17:256–65.
[25] (a) Shin YK, Brunschwig BS, Creutz C, Sutin N. J Phys Chem 1996;100:8157–69;
(b) Coe BJ, Harris JA, Brunschwig BS. J Phys Chem A 2002;106:897–905.
[26] (a) Gawinecki R, Trzebiatowska K. Pol J Chem 2001;75:231–9;
(b) Gawinecki R, Trzebiatowska K. Dyes Pigments 2000;45:103–7;
(c) Bajorek A, Trzebiatowska K, Jedrzejewska B, Pietrzak M, Gawinecki R, Paczkowski J. J Fluorescence 2004;14:295–307.
[27] (a) Wade JR, Etherington T, Folkard CW. Eur Pat Appl, 1991. 28p. CODEN: EPXXDW EP 419095 A2 19910327. (b) Coull JM, Stern AM, Haff LA, Fox BS, Huang Y. PCT Int Appl, 2006. 121p. CODEN: PIXXD2 WO 2006128138 A2 20061130.
[28] (a) Fidelman JG. US 3114635 19631217, 1963. 4p. (b) Wade JR, Etherington T, Folkard CW. Eur Pat Appl, 1991. 28p. CODEN: EPXXDW EP 419095 A2 19910327. (c) Chang Y-T, Rosania G. US Pat Appl Publ, 2005. 21p. Cont. of U.S. Ser. No. 656,875. CODEN: USXXCO US 2005054006 A1 20050310.
[29] Kwon O, Barlow S, Odom SA, Beverina L, Thompson NJ, Zojer E, et al. J Phys Chem A 2005;109:9346–52.
[30] (a) Dunlop R, Hardy ADU, Mills HH, Mackenzie RK, Macnicol DD, Williams DAR. J Chem Res 1979:152–3;
(b) Böhme U, Hartmann H, Görlitz G. Z Kristallogr 1996;211:133–4;
(c) Yagi S, Hyodo Y, Matsumoto S, Takahashi N, Kono H, Nakazumi H. J Chem Soc Perkin Trans 1 2000:599–603;
(d) Krygowski TM, Pindelska E, Anulewicz-Ostrowska R, Nowacki J. Pol J Chem 2002;76:1249–54;
(e) Jones PG, Dix I. Private communication, 2004; CCDC deposition number 241148. (f) Wang H, Lu Z-K, Lord SJ, Willets KA, Bertke JA, Bunge SF, et al. Tetrahedron 2007;63:103–14;
(g) Jiang X, Yang X-C, Zhao C-Z, Jin K, Sun L-C. J Phys Chem C 2007;111:9595–602.
[31] Selected examples: (a) Chinnakali K, Selladurai S, Sivakumar S, Subramanian K, Natarajan S. Acta Crystallogr Sect C 1990;46:835–7;
(b) Yip B-C, Moo F-M, Lok K-S, Fun H-K, Sivakumar K. Acta Crystallogr Sect C 1996;52:477–81;
(c) Honda T, Fujii I, Hirayama N, Aoyama N, Miike A. Acta Crystallogr Sect C 1996;52:364–5;
(d) Jasinski JP, Li Y. Acta Crystallogr Sect E 2002;58:o1312–4.
[32] Early examples: (a) Marder SR, Perry JW, Tiemann BG, Gorman CB, Gilmour S, Biddle SL, et al. J Am Chem Soc 1993;115:2524–6;
(b) Gorman CB, Marder SR. Proc Natl Acad Sci USA 1993;90:11297–301;
(c) Bourhill G, Brédas J-L, Cheng L-T, Marder SR, Meyers F, Perry JW, et al. J Am Chem Soc 1994;116:2619–20;
(d) Meyers F, Marder SR, Pierce BM, Brédas J-L. J Am Chem Soc 1994;116:10703–14.
[33] (a) Ulman A. An introduction to ultrathin organic films: from Langmuir–-Blodgett to self-assembly. Academic Press; 1991;
(b) Petty MC. Langmuir–Blodgett films: an introduction. Cambridge University Press; 1996;
(c) Ashwell GJ. J Mater Chem 1999;9. 1991–2003.
[34] See for examples: (a) Kim HS, Sohn KW, Jeon Y, Min H, Kim D, Yoon KB. Adv Mater 2007;19:260–3;
(b) Cariati E, Macchi R, Roberto D, Ugo R, Galli S, Casati N, et al. J Am Chem Soc 2007;129:9410–20.
[35] Whitesell JK, Davis RE, Saunders LL, Wilson RJ, Feagins JP. J Am Chem Soc 1991;113:3267–70.